

# A Few Topics **in the** Neutron Stars

**Myung-Ki Cheoun**

***Astro Nuclear Physics Group***  
***Soongsil University, Seoul, Korea***  
***<http://ssanp.ssu.ac.kr>***

**HaPhy, "Nuclear Physics in Various Environments"**  
**18-19 Oct., 2018, APCTP, Pohang**

# Contents I

0. Introduction : **Exotic matter**, **Symmetry Energy**, EoS...

1. Roles of **hyperons** in **RMF+QMC** models for Dense Matter  
1-1. Hartree-**Fock** Approximation  
1-2. **With QMC Model**

2. **Modified** Gravity and **Magnetic field** in Neutron Stars  
2-1. Modified TOV  
2-2. Magnetic field

**MKC et.al, PRC 82, 025804, (2010); PRC 83, 018802 (2011); JCAP 10, 21 (2013)...**

3. Other properties in Neutron Stars

**PRD 86 (2012) 123003 ; PRD83 (2011) 081303; PRC (2014)...**

4. Summary and Conclusions

# Contents II

## 0. Introduction

### 1. **Tidal Deformation from GW by Neutron Star Merge**

1-1. Tidal Deformation from GW

1-2. **Results** by Various Models for NS

### 2. **A Hybrid model for Neutron Star**

2-1. **Many-Body Interactions in Dense Matter**

2-2. **Hyperon Puzzles** of Neutron Stars

2-3. **Pomeron Exchange Model with SHF sets of Neutron Stars**

### 3. **Quark cluster star**

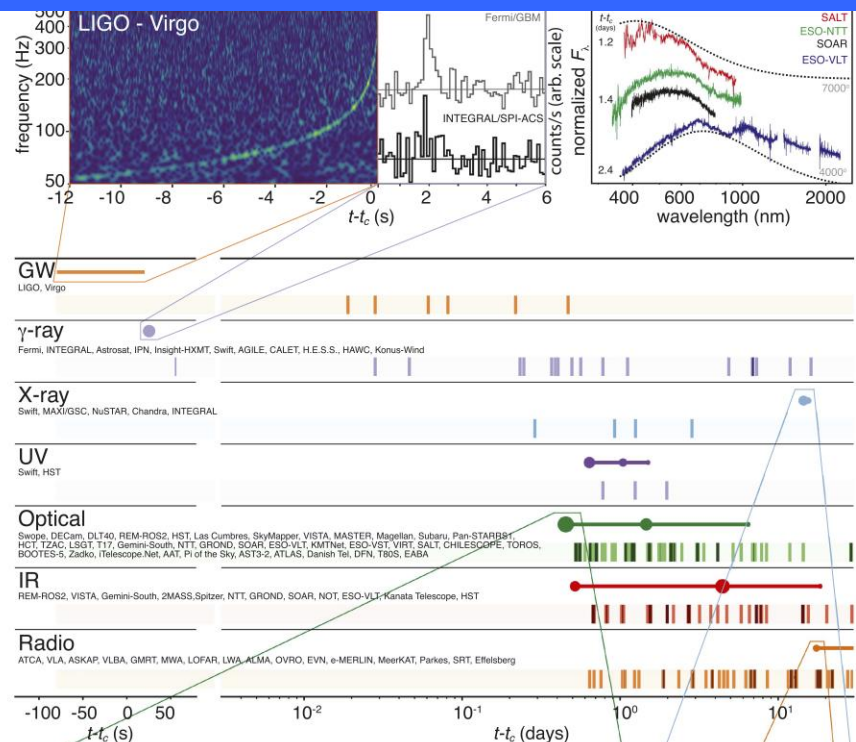
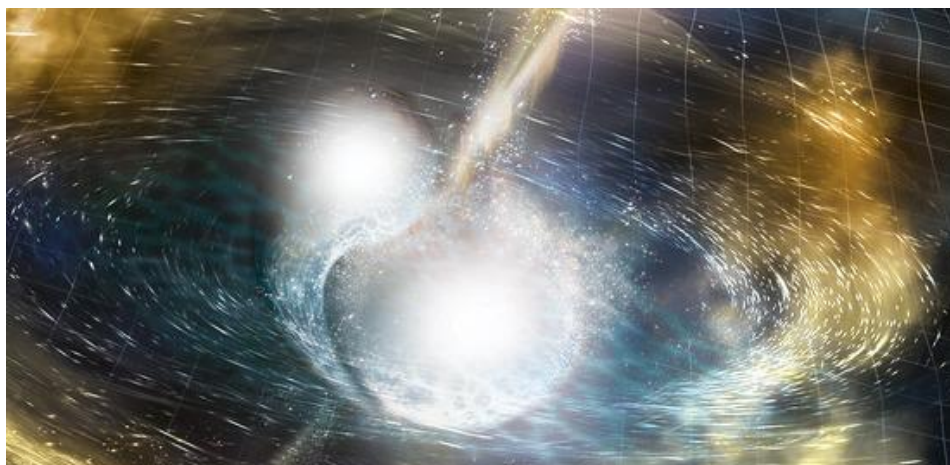
3-1. Quark Matter inside Neutron Star

3-2. **Quark Star and Quark Cluster Star**

## 4. Summary and Conclusions

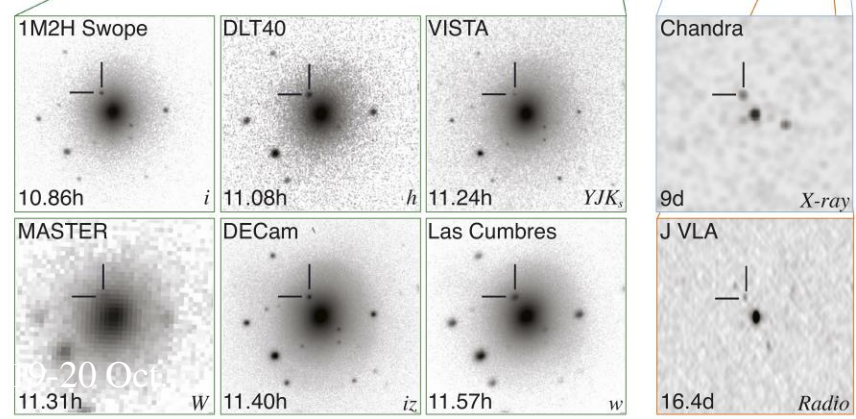
# Seen in LIGO + 70 Observatories

GW170817/GRB170817A/  
SSS17a



The EM **kilonova** indicates evidence of r-process nucleosynthesis that has implications for galactic chemical evolution and the **nuclear physics** of heavy nuclei.

HaPhy, APCTP, Poh 2018



# Deduced properties for GW170817

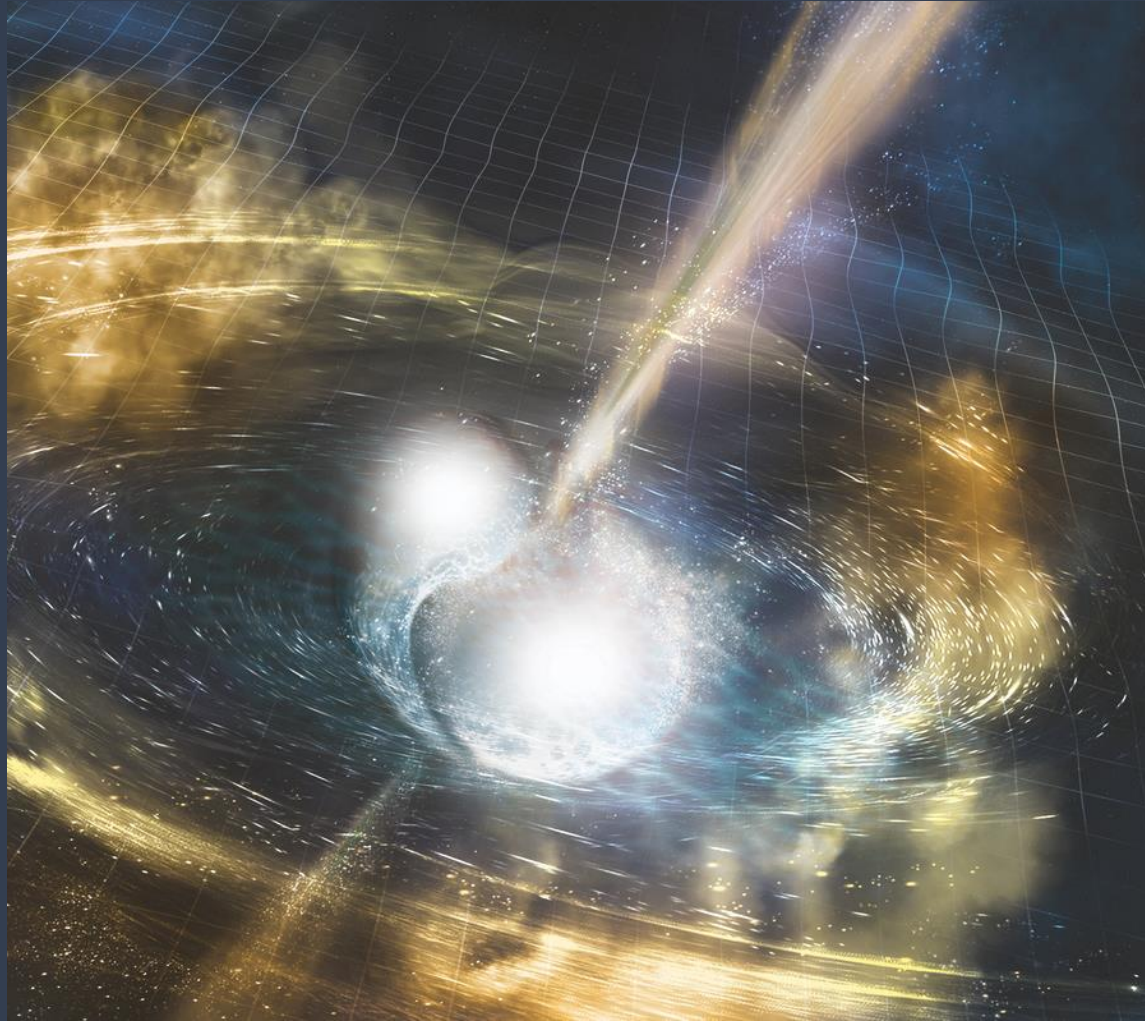
TABLE I. Source properties for GW170817: we give ranges encompassing the 90% credible intervals for different assumptions of the waveform model to bound systematic uncertainty. The mass values are quoted in the frame of the source, accounting for uncertainty in the source redshift.

	Low-spin priors ( $ \chi  \leq 0.05$ )	High-spin priors ( $ \chi  \leq 0.89$ )
Primary mass $m_1$	1.36–1.60 $M_\odot$	1.36–2.26 $M_\odot$
Secondary mass $m_2$	1.17–1.36 $M_\odot$	0.86–1.36 $M_\odot$
Chirp mass $\mathcal{M}$	1.188 $^{+0.004}_{-0.002}$ $M_\odot$	1.188 $^{+0.004}_{-0.002}$ $M_\odot$
Mass ratio $m_2/m_1$	0.7–1.0	0.4–1.0
Total mass $m_{\text{tot}}$	2.74 $^{+0.04}_{-0.01}$ $M_\odot$	2.82 $^{+0.47}_{-0.09}$ $M_\odot$
Radiated energy $E_{\text{rad}}$	$> 0.025 M_\odot c^2$	$> 0.025 M_\odot c^2$
Luminosity distance $D_L$	40 $^{+8}_{-14}$ Mpc	40 $^{+8}_{-14}$ Mpc
Viewing angle $\Theta$	$\leq 55^\circ$	$\leq 56^\circ$
Using NGC 4993 location	$\leq 28^\circ$	$\leq 28^\circ$
Combined dimensionless tidal deformability $\Lambda$	$\leq 800$	$\leq 700$
Dimensionless tidal deformability $\Lambda(1.4M_\odot)$	$\leq 800$	$\leq 1400$

Two  $\sim 1.4 M_\odot$  neutron stars 40 Mpc distant



# Introduction (GW170817)



Mass

$$m_1 = 1.36 - 1.60M_{\odot}$$

$$m_2 = 1.17 - 1.36M_{\odot}$$

Distance

$$40^{+8}_{-14} Mpc$$

Combined dimensionless  
tidal deformability

$$\tilde{\Lambda} \leq 800$$

Dimensionless  
tidal deformability

$$\Lambda(1.4M_{\odot}) \leq 800$$

NSF/LIGO/Sonoma State University/A. Simonnet

<https://www.ligo.caltech.edu/image/ligo20171016d>

PRL 119 161101 (2017)

# Introduction

$$Q = -\lambda \varepsilon$$

$Q$  : Quadrupole moment of neutron star

$\varepsilon$  : External quadrupole tidal field

$\lambda$  : a constant which is related to the tidal deformability  $\Lambda$

$$\Lambda = \frac{5}{2} \lambda \frac{1}{M} \left( \frac{c^2}{G} \right)^5$$

$$\tilde{\Lambda} = \frac{16}{13} \frac{(m_1 + 12m_2)m_1^4\Lambda_1 + (m_2 + 12m_1)m_2^4\Lambda_2}{(m_1 + m_2)^5}$$

# Tidal deformability

If we consider a static, spherically symmetric star of mass ( $m$ ) placed in a time-independent external quadrupole tidal field.

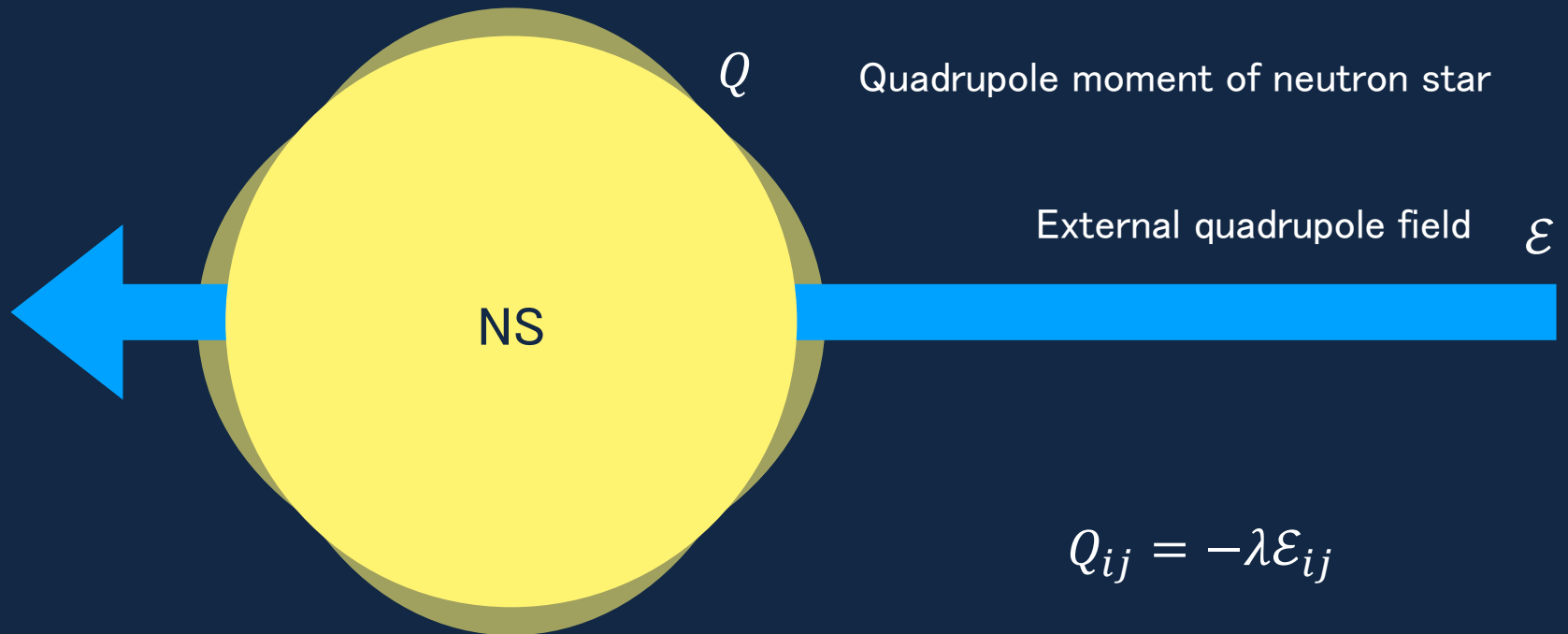
The star will develop in response a quadrupole moment





# Tidal deformability

If we consider a static, spherically symmetric star of mass ( $m$ ) placed in a time-independent external quadrupole tidal field, the star will develop in response a quadrupole moment



# Tidal deformability & Masses

$\lambda$  : a constant which is related to the tidal deformability  $\Lambda$

$$\Lambda = \frac{5}{2} \lambda \frac{1}{M} \left(\frac{c^2}{G}\right)^5$$

$$\Lambda \leq 800$$

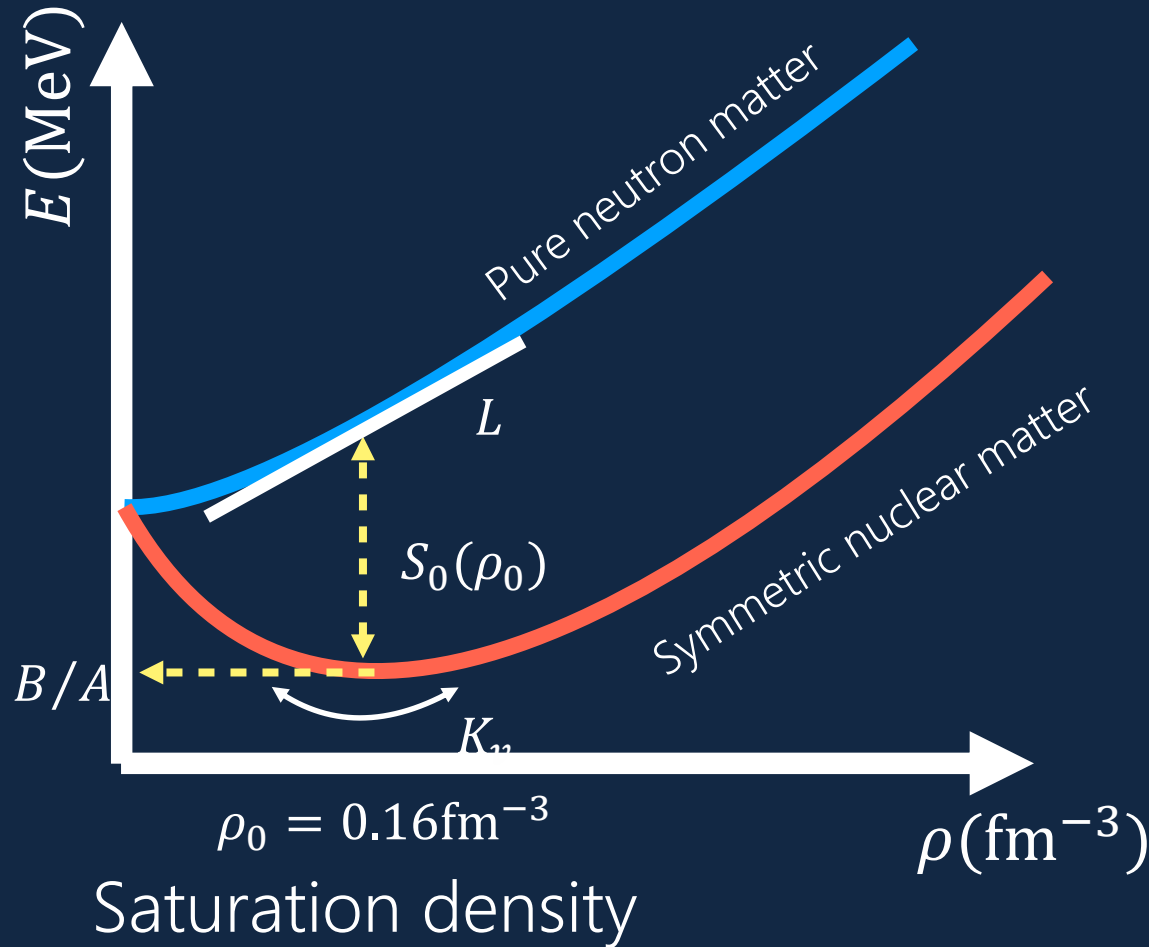
PRL 119 161101 (2017)

$$1.94M_{\odot} \leq M_{\text{NS}} \leq 2.01M_{\odot}$$

Nature 467 1081-1083  
(2010)

By using these observation data,  
we can give the constraint on **slope parameter and incompressibility**.

# Saturation properties present



Binding energy

$$B/A \approx -16.0 \text{ MeV}$$

Symmetry energy

$$S_0(\rho_0) = 32.5 \pm 0.5 \text{ MeV}^{[1]}$$

Slope parameter

$$L = 50 - 100 \text{ MeV}^{[2]}$$

Incompressibility

$$K = 180 - 260 \text{ MeV}^{[3]}$$

Effective mass

$$m^*/m = 0.7 - 0.8 \quad [4]$$

<sup>[1]</sup>PRL 108 052501 (2012) <sup>[3]</sup>PLB 778 207212 (2018)

<sup>[2]</sup>PRL 102 122501 (2009) <sup>[4]</sup>Nucl. Phys. A 950 64109 (2016)

# The effect of L and K on neutron stars

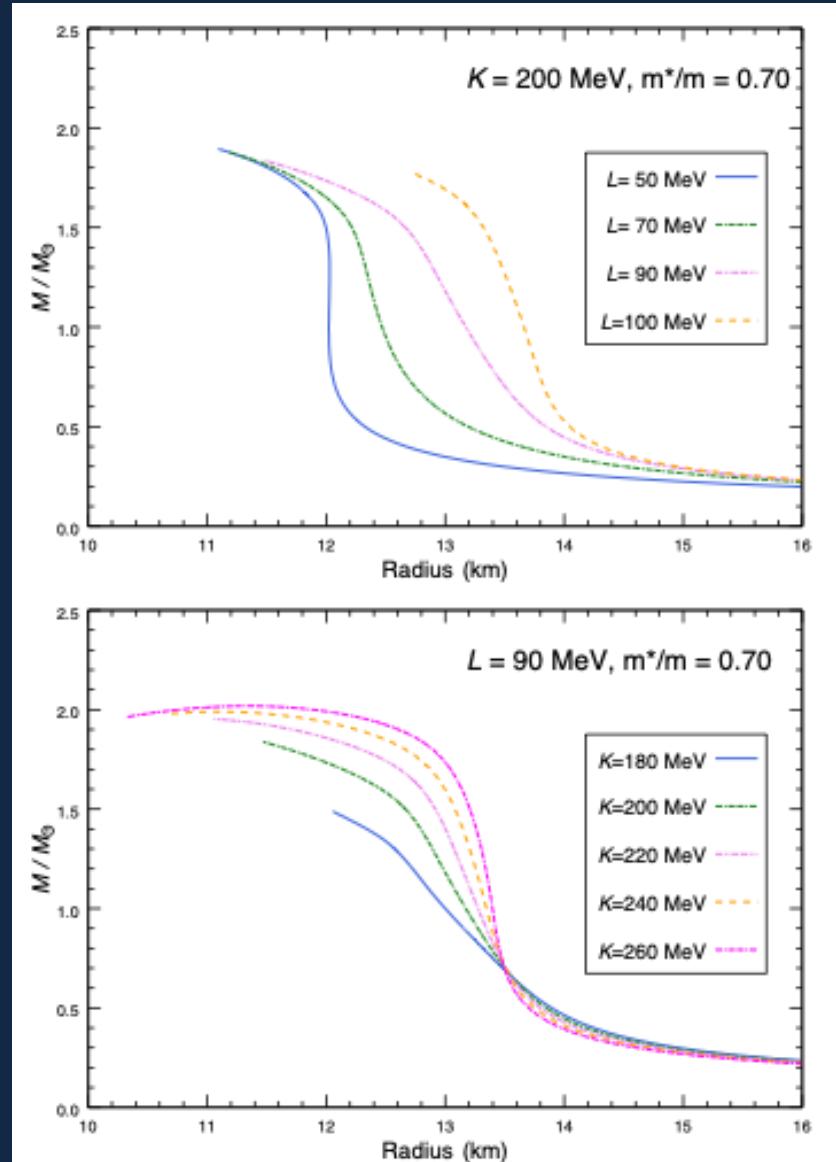
In these range,

$$L = 50 - 100 \text{ MeV} \quad K = 180 - 260 \text{ MeV}$$

neutron stars can cover wide range of mass and radius.

$$R(1.4M_{\odot}): 12 - 14 \text{ km}$$

$$\text{Maximum mass : } 1.5 - 2.1M_{\odot}$$



# Relativistic mean field model

Lagrangian density for static uniform nuclear matter :

$$\mathcal{L} = \sum_B \bar{\psi}_B [i\gamma_\mu \partial^\mu - M_B^*(\sigma_0, \sigma_0^*) - g_{\omega B} \gamma_0 \omega_0 - g_{\phi B} \gamma^0 \phi^0 - g_{\rho B} \gamma^0 \rho_0 I_{3B}] \psi_B - \frac{1}{2} m_\sigma^2 \sigma_0^2 - \frac{1}{2} m_{\sigma^*}^2 \sigma_0^{*2} + \frac{1}{2} m_\omega^2 \omega_0^2 + \frac{1}{2} m_\phi^2 \phi_0^2 + \frac{1}{2} m_\rho^2 \rho_0^2 - U_{NL}(\sigma_0, \omega_0, \rho_0)$$

$B = N, \Lambda, \Sigma^{+,0,-}, \Xi^{0,-}$

The effective baryon mass in matter :

$$M_B^*(\sigma, \sigma^*) = M_B - g_{\sigma B} \sigma - g_{\sigma^* B} \sigma^*$$

The following non-linear term is also introduced in order to reproduce the saturation properties of nuclear matter :

$$U_{NL}(\sigma, \omega^\mu, \rho^\mu) = \frac{1}{3} g_2 \sigma^3 + \frac{1}{4} g_3 \sigma^4 - \Lambda_v g_{\omega B}^2 g_{\rho B}^2 (\omega_0^2 \rho_0^2)$$



# Coupling constants

Coupling constants,  $g_{\sigma N}$ ,  $g_{\omega N}$ , and  $g_{\rho N}$  are determined so as to reproduce the binding energy per nucleon, and symmetry energy at saturation density.

$$B/A = -16.0\text{MeV} \quad \rho_0 = 0.16\text{fm}^{-3}$$
$$S_0(\rho_0) = 32.5\text{MeV}$$

The SU(3) symmetry in the vector-meson gives the relations of the coupling constants as

$$g_{\omega\Lambda} = g_{\omega\Sigma} = \frac{1}{1 + \sqrt{3}z\tan\theta_v} g_{\omega N} \quad g_{\rho\Sigma} = 2g_{\rho N}, g_{\rho\Xi} = g_{\rho N}, g_{\rho\Lambda} = 0$$

$$g_{\omega\Xi} = \frac{1 - \sqrt{3}z\tan\theta_v}{1 + \sqrt{3}z\tan\theta_v} g_{\omega N} \quad g_{\phi\Lambda} = g_{\phi\Sigma} = \frac{-\tan\theta_v}{1 + \sqrt{3}z\tan\theta_v} g_{\omega N} \quad g_{\phi\Xi} = -\frac{\sqrt{3}z + \tan\theta_v}{1 + \sqrt{3}\tan\theta_v} g_{\omega N}$$

$$g_{\phi N} = \frac{\sqrt{3}z - \tan\theta_v}{1 + \sqrt{3}z\tan\theta_v} g_{\omega N}$$

In the present calculation, we refer to the Nijmegen extended-soft-core (ESC) model [1] to fix the mixing angle ( $\theta_v$ ) and  $z$  as

$$\theta = 37.50^\circ, z = 0.1949$$

[1] Prog. Theor. Phys. Suppl. 185 14 (2010)

# Coupling constants

We need to consider the hyperon coupling. The  $\sigma$ -Y and  $\sigma^*$ -Y are determined as follows. The potential for hyperon Y in symmetric nuclear matter is calculated as

$$U_Y^{(N)} = -g_{\sigma Y}\sigma_0 + g_{\omega Y}\omega_0$$

$$U_{\Lambda}^{(N)} = -28\text{MeV}^{[1]} \quad U_{\Sigma}^{(N)} = 30\text{MeV}^{[2]} \quad U_{\Xi}^{(N)} = -18\text{MeV}^{[3]}$$

The potential for Y in Y-hyperon matter is written as :

$$U_Y^{(Y)} = -g_{\sigma Y}\sigma_0^{(Y)} - g_{\sigma^* Y}\sigma_0^{*(Y)} + g_{\omega Y}\omega^{(Y)} + g_{\phi Y}\phi_0^{(Y)}$$

$$U_{\Xi}^{(\Xi)} \simeq U_{\Lambda}^{(\Xi)} \simeq 2U_{\Xi}^{(\Lambda)} \simeq 2U_{\Lambda}^{(\Lambda)} [3] \quad U_{\Lambda}^{(\Lambda)} = -5\text{MeV} \quad \text{Nagara event}$$

# Non-Linear potential

We add the following NL potential to the Lagrangian density

$$U_{\text{NL}}(\sigma, \omega^\mu, \rho^\mu) = \frac{1}{3} g_2 \sigma^3 + \frac{1}{4} g_3 \sigma^4 - \Lambda_\nu g_{\omega B}^2 g_{\rho B}^2 (\omega_0^2 \rho_0^2)$$

Investigated range of incompressibility ( $K$ ), and the slope parameter ( $L$ ) at saturation density is

$$K = 180 - 260 \text{ MeV}$$

$$L = 50 - 100 \text{ MeV.}$$

We fix the effective mass ratio as

$$m^*/m = 0.7$$

# Result

## (Dependence on slope parameter)

- The slope parameter does not affect the maximum mass of neutron star.

- Around the 1.3 solar mass neutron star

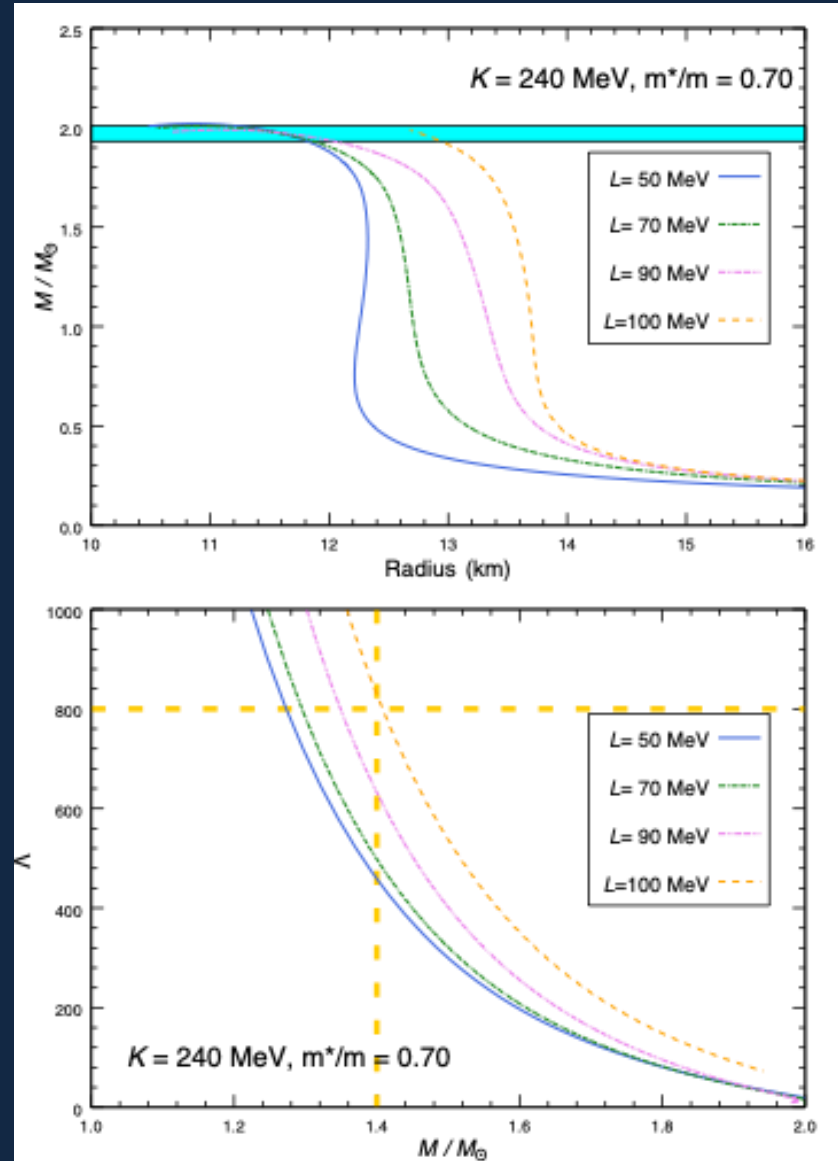
Slope parameter  $\longrightarrow$  Large

Radius  $\longrightarrow$  Large

- In the tidal deformability case, **the large slope parameter gives the higher tidal deformability.**

The onset of Lambda particle  $K_V = 240 \text{ MeV}$

	$L = 50 \text{ MeV}$	$70 \text{ MeV}$	$90 \text{ MeV}$	$100 \text{ MeV}$
$\rho_\Lambda$	0.450	0.440	0.410	0.380



# Result

## (Dependence on slope parameter)

- The slope parameter does not affect the maximum mass of neutron star.

- Around the 1.3 solar mass neutron star

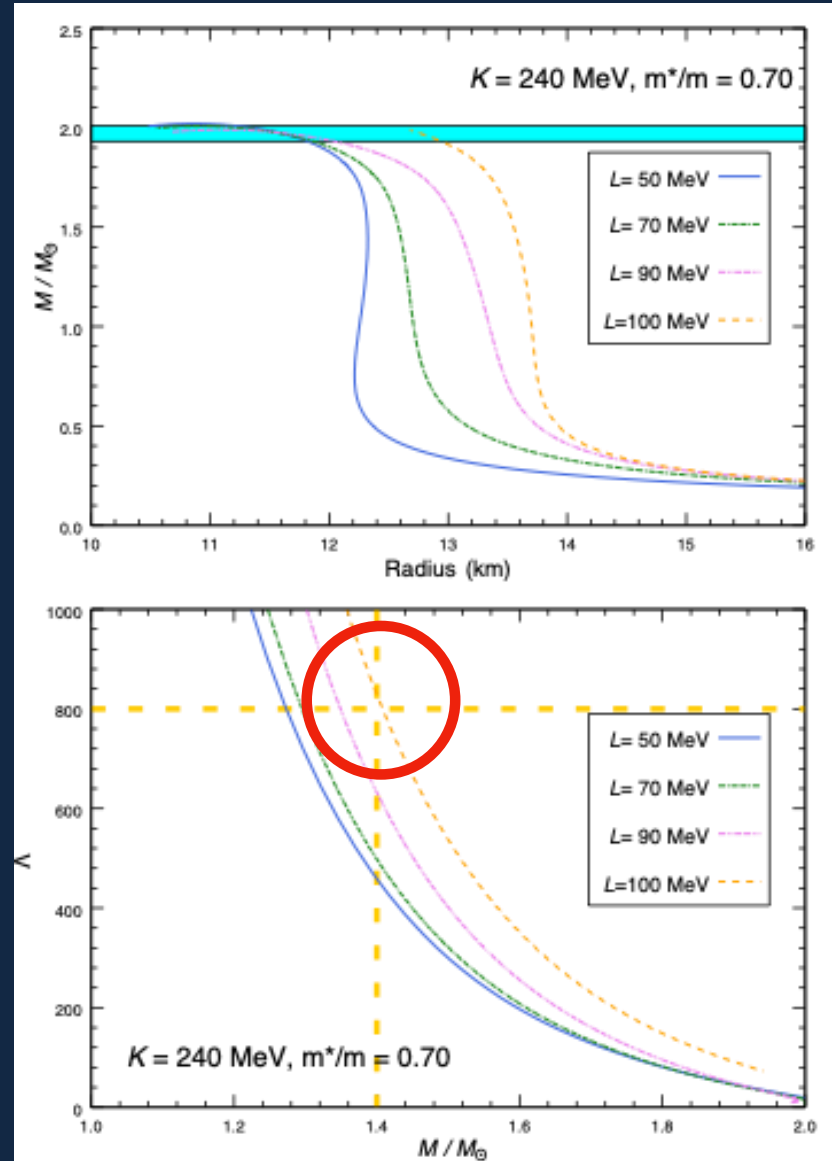
Slope parameter  $\longrightarrow$  Large

Radius  $\longrightarrow$  Large

- In the tidal deformability case, the large slope parameter gives the higher tidal deformability.

The onset of Lambda particle  $K_V = 240$  MeV

	L = 50 MeV	70 MeV	90 MeV	100 MeV
$\rho_\Lambda$	0.450	0.440	0.410	0.380





# Result

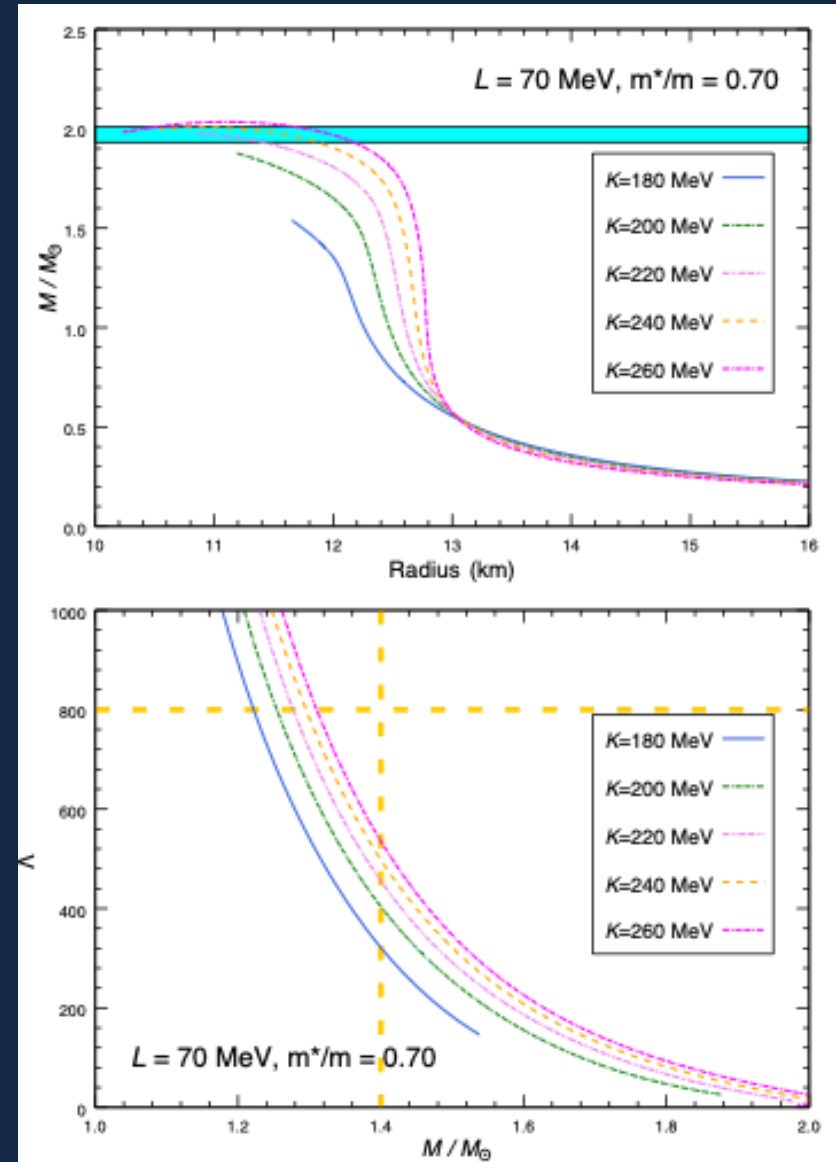
## (Dependence on incompressibility)

- The incompressibility affects both maximum mass and radius.

Incompressibility  $\longrightarrow$  Large

maximum mass  $\longrightarrow$  Large

- The two-solar mass neutron star cannot be described in  $K = 180$  and  $200$  MeV cases.



# Result

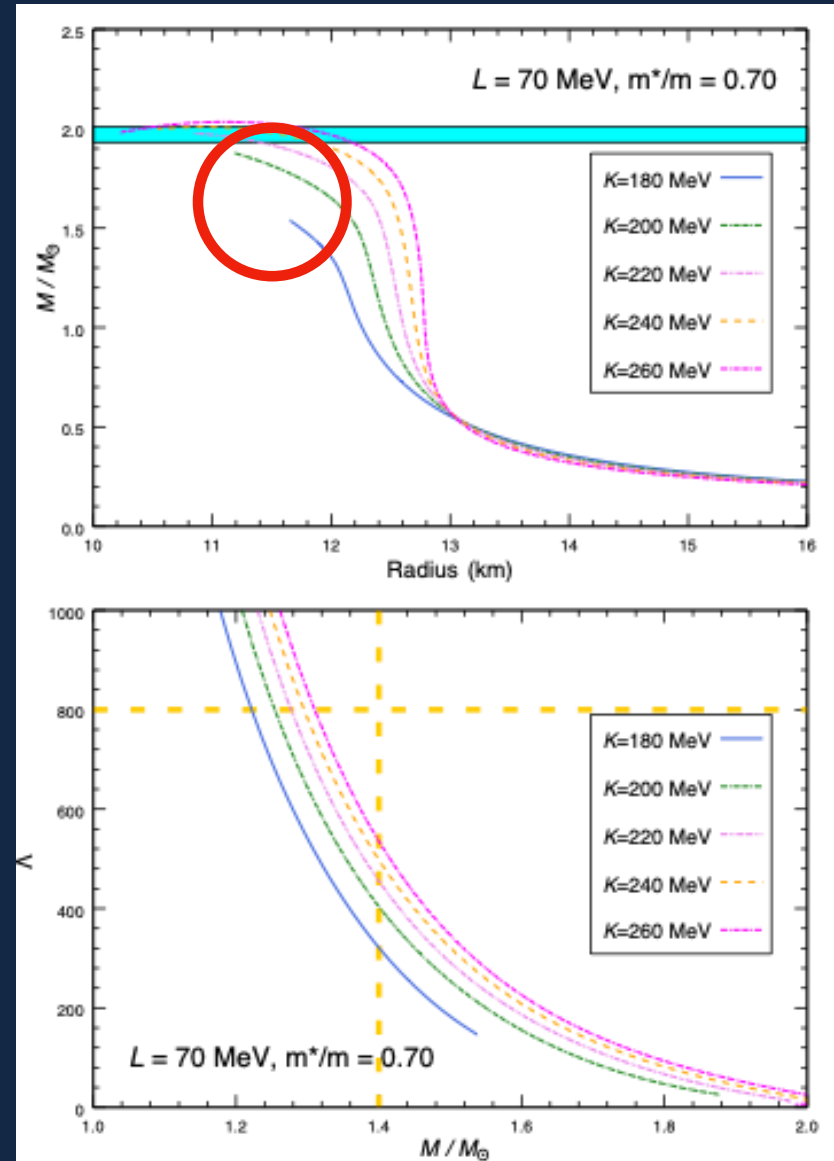
## (Dependence on incompressibility)

- The incompressibility affects both maximum mass and radius.

Incompressibility  $\longrightarrow$  Large

maximum mass  $\longrightarrow$  Large

- The two-solar mass neutron star cannot be described in  $K = 180$  and  $200$  MeV cases.



# Summary I

$m^*/m = 0.7$	$K = 180\text{MeV}$	$200\text{MeV}$	$220\text{MeV}$	$240\text{MeV}$	$260\text{MeV}$
$L = 50\text{MeV}$	×	×	○	○	○
$70\text{MeV}$	×	×	○	○	○
$90\text{MeV}$	×	×	○	○	○
$100\text{MeV}$	×	×	×	×	×

- We changed the slope parameter and incompressibility by using RMF model with non-linear potential.
- The slope parameter affects the radius and tidal deformability.
- The incompressibility can change the maximum mass of the neutron star.
- Neutron stars prefer the high incompressibility and low slope parameter.
- **We can reduce the ambiguity of slope parameter and incompressibility by using the astronomical observation data.**

# Contents

## 0. Introduction

### 1. **Tidal Deformation from GW by Neutron Star Merge**

1-1. Tidal Deformation from GW

1-2. **Results** by Various Models for NS

### 2. **A Hybrid model for Neutron Star**

2-1. **Many-Body Interactions in Dense Matter**

2-2. **Hyperon Puzzles** of Neutron Stars

2-3. **Pomeron Exchange Model with SHF sets of Neutron Stars**

### 3. **Quark cluster star**

3-1. Quark Matter inside Neutron Star

3-2. **Quark Star and Quark Matter Star**

### 4. Summary and Conclusions

# Interaction between particles

		Two-body			Three-body			
	Type	NN	NY	YY	NNN	NNY	NYY	YYY
Y.Lim et al.,[1]	SHF	Skyrme interaction					-	-
Y. Yamamoto et al.,[2]	BHF	BHF	BHF( $\Lambda\Sigma E$ )	BHF( $\Lambda\Lambda$ )	TBR+TBA [2]			
<b>Ours</b>	<b>Hybrid</b>	<b>SHF</b>	<b>BHF(<math>\Lambda\Sigma E</math>)</b>	<b>BHF(<math>\Lambda\Lambda</math>)</b>	<b>SHF</b>	<b>TBR+TBA [2]</b>		

We suggest a hybrid model

- The  **$NN$  interactions** are described by the Skyrme-Hartree-Fock (SHF) [SkI4, SG1, SLy4]
- The **hyperon interactions** are treated by taking the Brueckner-Hartree-Fock approach (BHF)

## Skyrme-Hartree-Fock approach

- Effective potential in the nuclear matter

## Brueckner-Hartree-Fock approach

- Extending two-body interaction in free space to two-body interaction in matter



# Interaction between particles

		Two-body			Three-body			
	Type	NN	NY	YY	NNN	NNY	NYY	YYY
Y.Lim et al.,[1]	SHF	Skyrme interaction					-	-
Y. Yamamoto et al.,[2]	BHF	BHF	BHF( $\Lambda\Sigma E$ )	BHF ( $\Lambda\Lambda$ )	TBR+TBA [2]			
<b>Ours</b>	<b>Hybrid</b>	<b>SHF</b>	<b>BHF(<math>\Lambda\Sigma E</math>)</b>	<b>BHF (<math>\Lambda\Lambda</math>)</b>	<b>SHF</b>	<b>TBR+TBA [2]</b>		

We suggest a hybrid model

- The  **$MN$  interactions** are described by the Skyrme-Hartree-Fock (SHF) [SkI4, SG1, SLy4]
- The **hyperon interactions** are treated by taking the Brueckner-Hartree-Fock approach (BHF)

If we use the SG1 for hybrid model, then we call H-SG1.

Type	$\rho_0$ (fm <sup>-3</sup> )	B/A (MeV)	$E_{\text{sym}}$ (MeV)	L (MeV)	$K_\infty$ (MeV)
SG1	0.155	-15.9	29	69	263
SkI4	0.160	-16.1	29	59	246
SLy4	0.160	-16	32	47	230
exp		-16	$\sim 30$	$54 \pm 19$	${}^3 230 \pm 30$

# Many-body interaction for hyperon

This ESC08 is used to consider two-body interaction.

The experimental nuclear saturation properties, the density  $\rho_N$ , the binding energy per nucleon  $E/A$ , the compression modulus  $K$ , cannot be reproduced quantitatively with nuclear two-body interactions only.

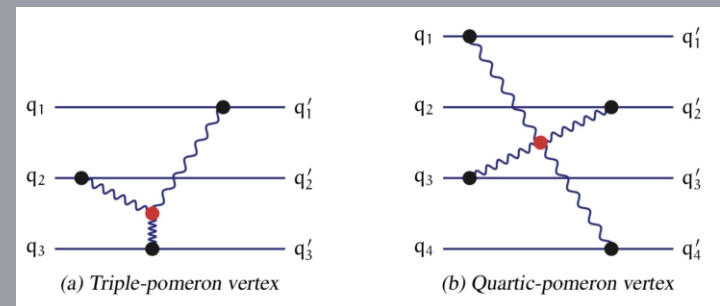
Generally, the  $N$ -body local potential  $W^{(N)}$  by pomeron exchange is

$$W^{(N)}(\mathbf{x}_1, \dots, \mathbf{x}_N) = g_P^{(N)} g_p^N \left( \int \frac{d^3 k_i}{(2\pi)^3} e^{-i\mathbf{k}_i \cdot \mathbf{x}_i} \right) (2\pi)^3 \left( \sum_{i=0}^N \mathbf{k}_i \right) \prod_{i=1}^N [\exp(-\mathbf{k}_i^2)] \cdot \mathcal{M}^{4-3N}$$

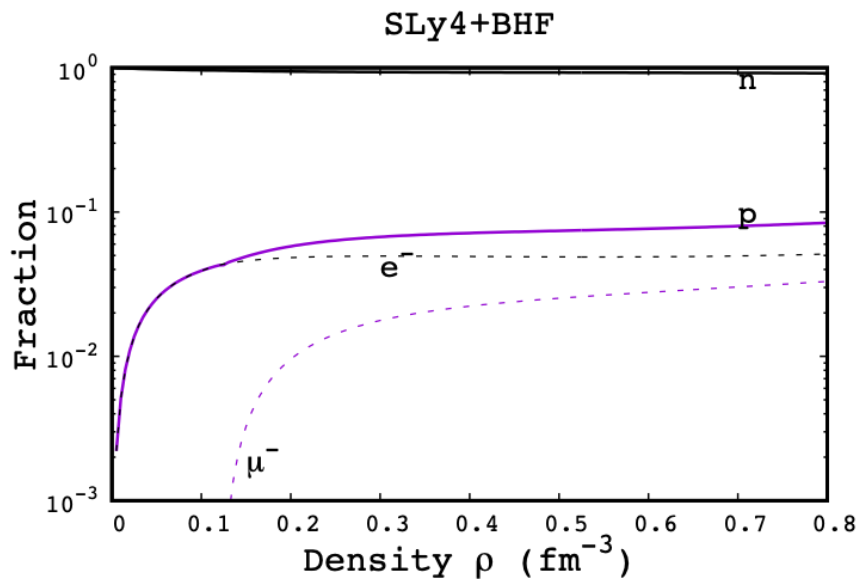
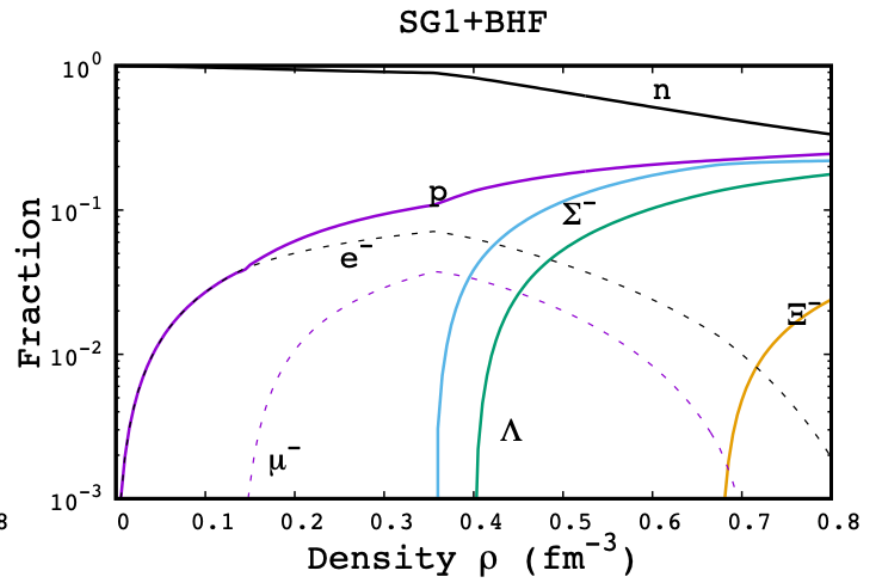
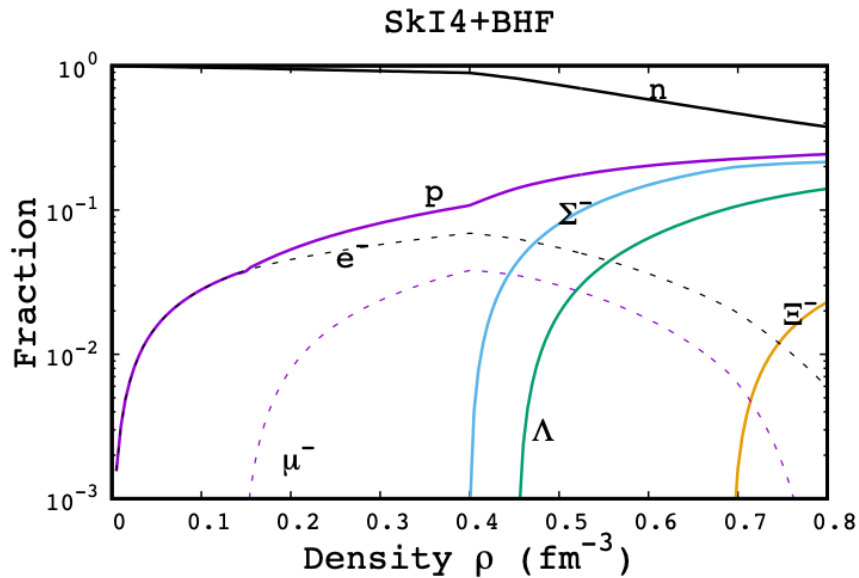
where  $g_p$  and  $g_p^{(N)}$  are the two-body and  $N$ -body pomeron strengths, respectively.

If we integrate the above equation by  $\mathbf{x}_3, \dots, \mathbf{x}_N$ , then

$$\begin{aligned} V_{\text{eff}}^{(N)}(\mathbf{x}_1, \mathbf{x}_2) &= \rho^{N-2} \int d^3 x_3 \dots \int d^3 x_N W^{(N)}(\mathbf{x}_1, \mathbf{x}_2, \dots, \mathbf{x}_N) \\ &= g_p^{(N)} g_p^N \frac{\rho^{N-2}}{\mathcal{M}^{3N-4}} \left( \frac{m_P}{\sqrt{2\pi}} \right)^3 \exp\left( -\frac{1}{2} m_P^2 r_{12}^2 \right) \end{aligned}$$



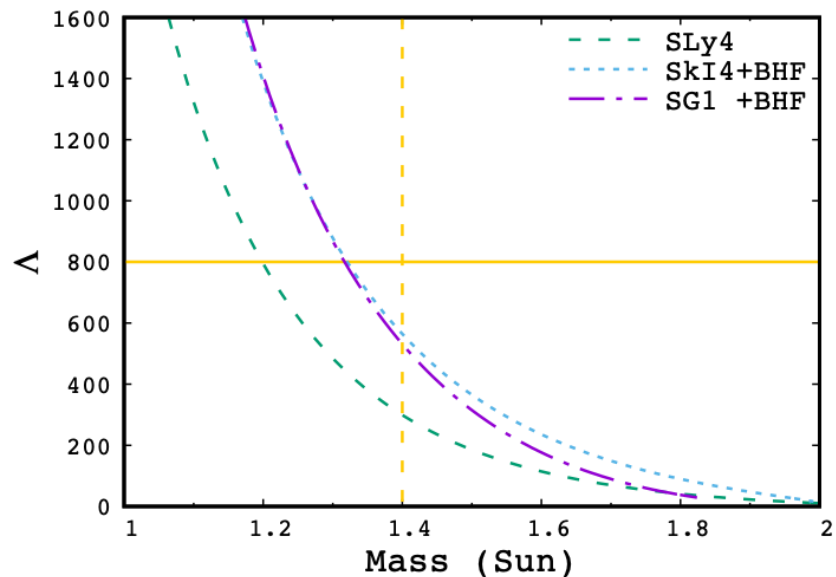
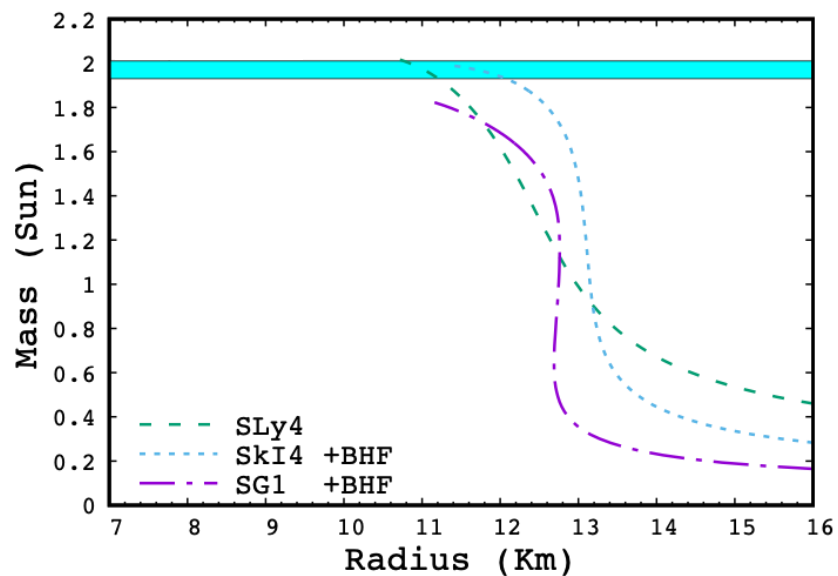
# Particle profile



If we input the center density, then  
we can obtain the neutron star properties

mass, radius and  $\Lambda$

# Mass-radius relation and tidal deformability

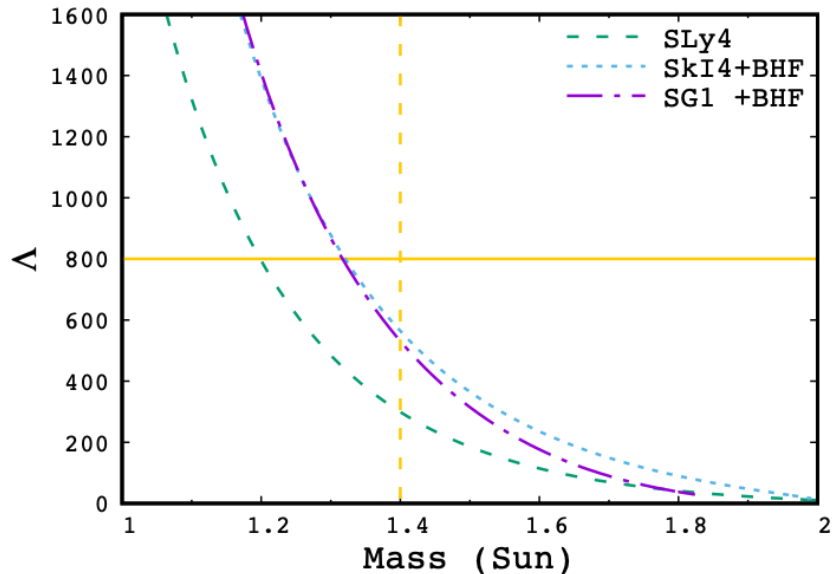
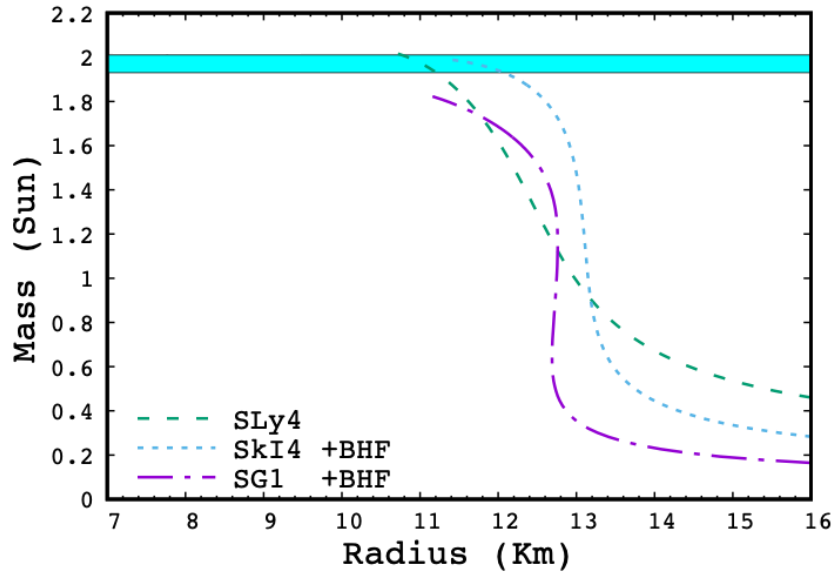


SkI4 + BHF case can reach  
the two-solar mass neutron star.

The same mass      The large  $\Lambda$

The pressure is large

# Mass-radius relation and tidal deformability



$$\begin{array}{l}
 m_1 = 1.36 - 1.60M_{\odot} \\
 m_2 = 1.17 - 1.36M_{\odot}
 \end{array}
 \longrightarrow
 \begin{array}{l}
 m_1 = 1.48M_{\odot} \\
 m_2 = 1.27M_{\odot}
 \end{array}$$

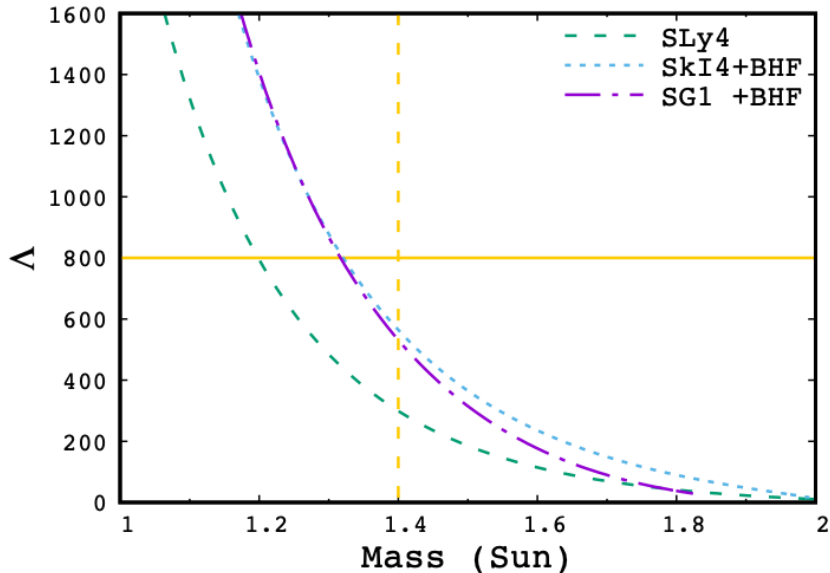
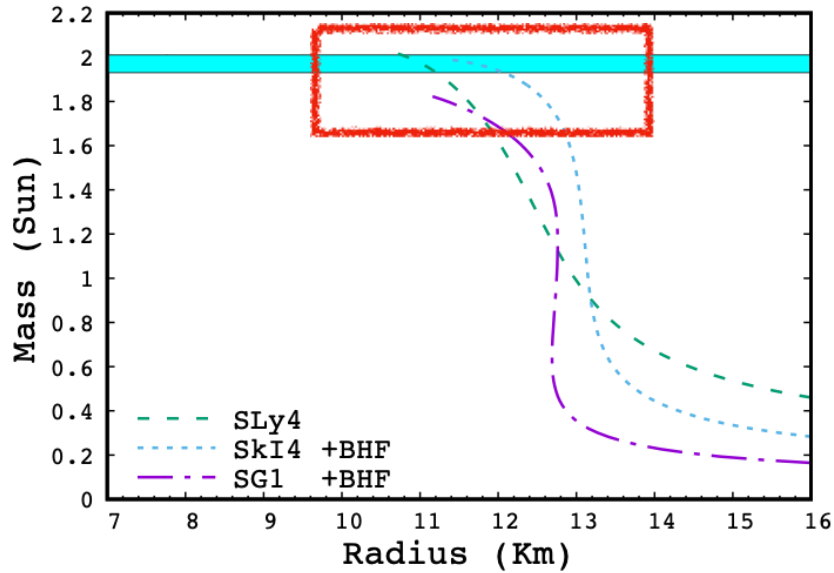
$$\tilde{\Lambda} = \frac{16(m_1 + 12m_2)m_1^4\Lambda_1 + (m_2 + 12m_1)m_2^4\Lambda_2}{(m_1 + m_2)^5}$$

preliminary

	$\Lambda_1$	$\Lambda_2$	$\tilde{\Lambda}$
SLy4	202	560	343
H-SkI4	400	980	629
H-SG1	345	1023	611

$$\tilde{\Lambda} \leq 800$$

# Mass-radius relation and tidal deformability



$$\begin{array}{l}
 m_1 = 1.36 - 1.60M_{\odot} \\
 m_2 = 1.17 - 1.36M_{\odot}
 \end{array}
 \longrightarrow
 \begin{array}{l}
 m_1 = 1.48M_{\odot} \\
 m_2 = 1.27M_{\odot}
 \end{array}$$

$$\tilde{\Lambda} = \frac{16(m_1 + 12m_2)m_1^4\Lambda_1 + (m_2 + 12m_1)m_2^4\Lambda_2}{(m_1 + m_2)^5}$$

preliminary

	$\Lambda_1$	$\Lambda_2$	$\tilde{\Lambda}$
SLy4	202	560	343
H-SkI4	400	980	629
H-SG1	345	1023	611

$$\tilde{\Lambda} \leq 800$$

# Summary II

- The density of neutron star is very high.  
hyperons can be generated in the core.
- The gravitational waves from binary neutron star merge gives the **tidal deformability** and masses of NS
- To get mass and tidal deformability,  
we need equation of state for neutron star.
- Our hybrid model can describe the **2 solar mass NS** and **measured tidal deformability**.

# Contents

## 0. Introduction

### 1. **Tidal Deformation from GW by Neutron Star Merge**

1-1. Tidal Deformation from GW

1-2. **Results** by Various Models for NS

### 2. **A Hybrid model for Neutron Star**

2-1. **Many-Body Interactions in Dense Matter**

2-2. **Hyperon Puzzles** of Neutron Stars

2-3. **Pomeron Exchange Model with SHF sets of Neutron Stars**

### 3. **Quark cluster star**

3-1. Quark Matter inside Neutron Star

3-2. **Quark Star and Quark Cluster Star**

### 4. Summary and Conclusions



## EQUATION OF STATE FOR NEUTRON STARS WITH HYPERONS AND QUARKS IN THE RELATIVISTIC HARTREE–FOCK APPROXIMATION

TSUYOSHI MIYATSU<sup>1</sup>, MYUNG-KI CHEOUN<sup>1</sup>, AND KOICHI SAITO<sup>2</sup>

<sup>1</sup> Department of Physics, Soongsil University, Seoul 156-743, Korea; tmiyatsu@ssu.ac.kr, cheoun@ssu.ac.kr

<sup>2</sup> Department of Physics, Faculty of Science and Technology, Tokyo University of Science, Noda 278-8510, Japan; koichi.saito@rs.tus.ac.jp

*Received 2015 June 16; accepted 2015 October 1; published 2015 November 9*

$$\mathcal{L}_H = \mathcal{L}_B + \mathcal{L}_M + \mathcal{L}_{\text{int}}, \quad (1)$$

where

$$\mathcal{L}_B = \sum_B \bar{\psi}_B (i\gamma_\mu \partial^\mu - M_B) \psi_B, \quad (2)$$

with  $\psi_B$  being the baryon field and  $M_B$  being the baryon mass in a vacuum. The sum  $B$  runs over the octet baryons: proton ( $p$ ), neutron ( $n$ ),  $\Lambda$ ,  $\Sigma^{+0-}$ , and  $\Xi^{0-}$ . For the free baryon masses, we take  $M_N = 939$  MeV,  $M_\Lambda = 1116$  MeV,  $M_\Sigma = 1193$  MeV, and  $M_\Xi = 1318$  MeV, respectively. Lepton Lagrangian is introduced in Section 4.

In the present calculation, we study the effects of direct and exchange contributions on hadronic matter through not only the exchanges of non-strange mesons ( $\sigma$ ,  $\omega$ ,  $\pi$ , and  $\rho$ ) but also those of strange mesons ( $\sigma^*$  and  $\phi$ ). Thus, the meson term reads

$$\begin{aligned} \mathcal{L}_M = & \frac{1}{2} (\partial_\mu \sigma \partial^\mu \sigma - m_\sigma^2 \sigma^2) + \frac{1}{2} (\partial_\mu \sigma^* \partial^\mu \sigma^* - m_{\sigma^*}^2 \sigma^{*2}) \\ & + \frac{1}{2} m_\omega^2 \omega_\mu \omega^\mu - \frac{1}{4} W_{\mu\nu} W^{\mu\nu} + \frac{1}{2} m_\phi^2 \phi_\mu \phi^\mu - \frac{1}{4} P_{\mu\nu} P^{\mu\nu} \\ & + \frac{1}{2} m_\rho^2 \rho_\mu \cdot \rho^\mu - \frac{1}{4} R_{\mu\nu} \cdot R^{\mu\nu} \\ & + \frac{1}{2} (\partial_\mu \pi \cdot \partial^\mu \pi - m_\pi^2 \pi^2), \end{aligned} \quad (3)$$

The interaction Lagrangian is given by

$$\begin{aligned} \mathcal{L}_{\text{int}} = & \sum_B \bar{\psi}_B \left[ g_{\sigma B}(\sigma) \sigma + g_{\sigma^* B}(\sigma^*) \sigma^* \right. \\ & - g_{\omega B} \gamma_\mu \omega^\mu + \frac{f_{\omega B}}{2\mathcal{M}} \sigma_{\mu\nu} \partial^\nu \omega^\mu \\ & - g_{\phi B} \gamma_\mu \phi^\mu + \frac{f_{\phi B}}{2\mathcal{M}} \sigma_{\mu\nu} \partial^\nu \phi^\mu - g_{\rho B} \gamma_\mu \rho^\mu \cdot \mathbf{I}_B \\ & \left. + \frac{f_{\rho B}}{2\mathcal{M}} \sigma_{\mu\nu} \partial^\nu \rho^\mu \cdot \mathbf{I}_B - \frac{f_{\pi B}}{m_\pi} \gamma_5 \gamma_\mu \partial^\mu \pi \cdot \mathbf{I}_B \right] \psi_B, \quad (7) \end{aligned}$$

$$g_{\sigma B}(\sigma) = g_{\sigma B} b_B \left[ 1 - \frac{a_B}{2} (g_{\sigma N} \sigma) \right], \quad (8)$$

$$g_{\sigma^* B}(\sigma^*) = g_{\sigma^* B} b'_B \left[ 1 - \frac{a'_B}{2} (g_{\sigma^* \Lambda} \sigma^*) \right], \quad (9)$$

where  $g_{\sigma N}$  and  $g_{\sigma^* \Lambda}$  are, respectively, the  $\sigma$ - $N$  and  $\sigma^*$ - $\Lambda$  coupling constants at zero density. The effect of the variation of baryon structure at the quark level can be described with the parameters  $a_B$  and  $a'_B$ . In addition, the extra parameters,  $b_B$  and  $b'_B$ , are necessary to express the effect of hyperfine interaction between two quarks (Nagai et al. 2008; Miyatsu & Saito 2009; Saito 2010). The couplings in the CQMC model are invariant

$$M_B^*(k) = M_B + \Sigma_B^s(k), \quad (12)$$

$$k_B^{*\mu} = (k_B^{*0}, \mathbf{k}_B^*) = (k^0 + \Sigma_B^0(k), \mathbf{k} + \hat{k} \Sigma_B^v(k)), \quad (13)$$

$$E_B^*(k) = [k_B^{*2} + M_B^{*2}(k)]^{1/2}. \quad (14)$$

### 3. QUARK MATTER DESCRIPTION

We briefly present a description of uniform quark matter. The thermodynamic potential can be simply expressed by (Freedman & McLerran 1978; Farhi & Jaffe 1984; Alcock et al. 1986; Haensel et al. 1986)

$$\Omega = \sum_q \Omega_q + B, \quad (41)$$

with the quark term,  $\Omega_q$ , and the bag constant,  $B$ . The sum  $q$  runs over three-flavor quarks ( $u$ ,  $d$ , and  $s$ ), and the quark thermodynamic potential is given by a sum of the kinetic term and the interaction term due to the OGE (Freedman & McLerran 1978):

$$\Omega_q = -\frac{g_q(2J_q + 1)}{24\pi^2} \left[ F(\mu_q, m_q) - \frac{2\alpha_c}{\pi} G(\mu_q, m_q) \right], \quad (42)$$

The quark number density is related to  $\Omega_q$  via  $\rho_q = -\partial\Omega_q/\partial\mu_q$ , and the baryon density and the charge density in quark matter are given by  $n_B = \frac{1}{3}\sum_q \rho_q$  and  $n_C = \frac{2}{3}\rho_u - \frac{1}{3}(\rho_d + \rho_s)$ , respectively. The energy density and pressure for quark matter are then written as

$$\varepsilon_Q = \sum_q (\Omega_q + \mu_q \rho_q) + B, \quad (45)$$

$$P_Q = -\sum_q \Omega_q - B. \quad (46)$$

Instead of hadronic matter, quark matter is expected to exist at very high densities such as at the center of a neutron star. However, the exact value of the transition density from hadron phase (HP) to quark phase is still unknown. In the present calculation, in order to study the effect of quark matter on neutron stars, we introduce a density-dependent bag constant, which is assumed to be given by a Gaussian parametrization (Burgio et al. 2002a, 2002b)

$$B(n_B) = B_\infty + (B_0 - B_\infty) \exp\left[-\beta\left(\frac{n_B}{n_0}\right)^2\right], \quad (47)$$

<sup>CTP, Po</sup>  
20..

THE ASTROPHYSICAL JOURNAL, 813:135 (13pp), 2015 November 10

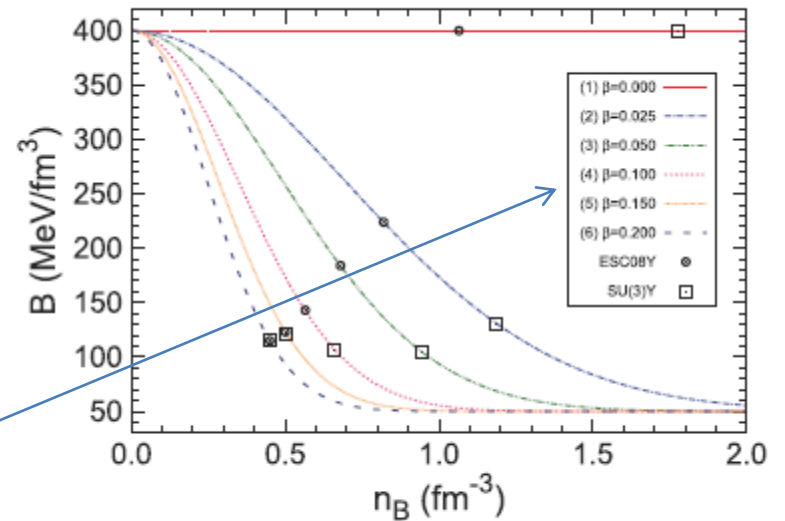


**Figure 6.** Density-dependence of bag constant given in Equation (47). The circles (squares) show the critical points in ESC08Y (SU(3)Y) (see also Table 6).

$$\mathcal{L}_\ell = \sum_\ell \bar{\psi}_\ell (i\gamma_\mu \partial^\mu - m_\ell) \psi_\ell, \quad (50)$$

with  $\psi_\ell$  being the lepton field and  $m_\ell$  being its mass. The sum  $\ell$  is for  $e^-$  and  $\mu^-$ . The lepton energy density, pressure, and number density are then given by

$$\epsilon_\ell = \sum_\ell \frac{2J_\ell + 1}{2\pi^2} \int_0^{k_{F_\ell}} dk k^2 \sqrt{k^2 + m_\ell^2}, \quad (51)$$

$$P_\ell = \frac{1}{3} \sum_\ell \frac{2J_\ell + 1}{2\pi^2} \int_0^{k_{F_\ell}} dk \frac{k^4}{\sqrt{k^2 + m_\ell^2}}, \quad (52)$$

$$\rho_\ell = \frac{2J_\ell + 1}{2\pi^2} \int_0^{k_{F_\ell}} dk k^2 = \frac{2J_\ell + 1}{6\pi^2} k_{F_\ell}^3, \quad (53)$$

where  $J_\ell$  is the spin degeneracy factor of lepton  $\ell$ . The total energy density and pressure for hadronic (quark) matter are given by the sum of the hadron (quark) and lepton parts, namely,  $\epsilon = \epsilon_{H(Q)} + \epsilon_\ell$  and  $P = P_{H(Q)} + P_\ell$ . Furthermore, the condition of  $\beta$  equilibrium is expressed as (Glendenning 1992, 2001; Maruyama et al. 2007)

$$\mu_n = \mu_\Lambda = \mu_{\Sigma^0} = \mu_{\Xi^0} = \mu_u + 2\mu_d, \quad (54)$$

$$\mu_n + \mu_e = \mu_{\Sigma^-} = \mu_{\Xi^-} = \mu_d = \mu_s, \quad (55)$$

$$\mu_n - \mu_e = \mu_p = \mu_{\Sigma^+}, \quad (56)$$

$$\mu_e = \mu_u, \quad (57)$$

In order to describe the coexistence of hadrons and quarks, we impose Gibbs criterion for chemical equilibrium (Glendenning 1992, 2001). Under Gibbs criterion, in the mixed phase (MP), pressure in the HP must balance with that in the quark phase (QP) to ensure mechanical stability as follows,

$$P_{\text{HP}}(\mu_n, \mu_e) = P_{\text{QP}}(\mu_n, \mu_e). \quad (58)$$

In the MP, where the condition, Equation (58), is satisfied, the charge neutrality can be expressed as

$$(1 - \chi)n_C^{\text{HP}} + \chi n_C^{\text{QP}} = 0, \quad (59)$$

with  $n_C^{\text{HP}}$  ( $n_C^{\text{QP}}$ ) being the charge density in the HP (QP), and  $\chi$  being a volume fraction for the QP. The total energy density and baryon number density in the MP are then given by

$$\epsilon_{\text{MP}} = (1 - \chi)\epsilon_{\text{HP}} + \chi\epsilon_{\text{QP}}, \quad (60)$$

$$n_B^{\text{MP}} = (1 - \chi)n_B^{\text{HP}} + \chi n_B^{\text{QP}}. \quad (61)$$

$$U_Y^{(B)} = \Sigma_Y^{sH} - \Sigma_Y^{0H} + \frac{1}{2M_Y} \left[ \Sigma_Y^{sH} - \Sigma_Y^{0H} \right]^2, \quad (63)$$

where  $\Sigma_Y^{s(0)H}$  is the direct term of the baryon self-energy for the scalar (the time component of the vector) part. Then, we can determine the coupling constants,  $g_{\sigma Y}$ , following the values of potential depth around  $n_0$  suggested from the experimental data of hypernuclei:  $U_\Lambda^{(N)} = -28$  MeV,  $U_\Sigma^{(N)} = +30$  MeV, and  $U_\Xi^{(N)} = -18$  MeV (Schaffner et al. 1994). The scalar strange coupling constants,  $g_{\sigma^* Y}$ , are restricted by the relation  $U_\Xi^{(\Xi)} \simeq U_\Lambda^{(\Xi)} \simeq 2U_\Xi^{(\Lambda)} \simeq 2U_\Lambda^{(\Lambda)}$  (Schaffner et al. 1994; Schaffner & Mishustin 1996; Yang & Shen 2008). We here take  $U_\Lambda^{(\Lambda)} \simeq -5$  MeV, which has been implied by the Nagara event (Takahashi et al. 2001).

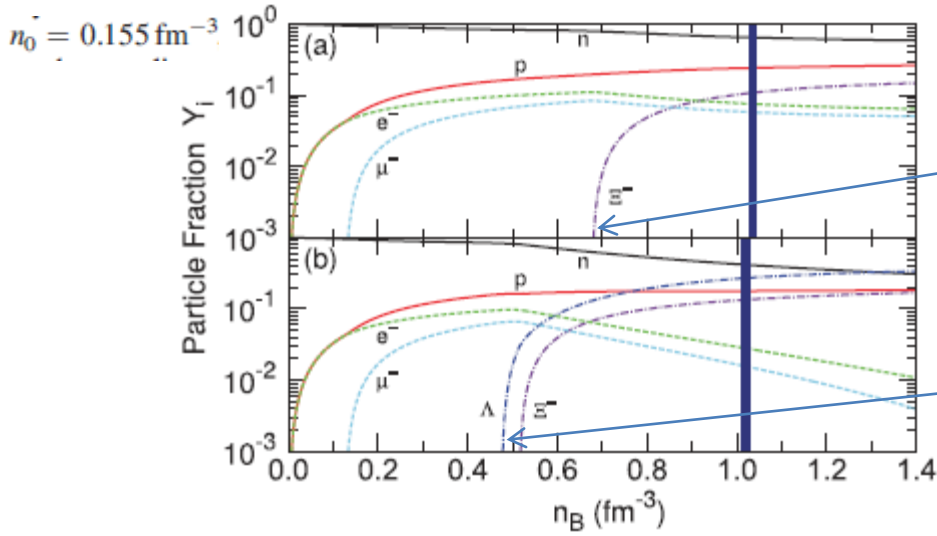


**Figure 1.** Particle fractions,  $Y_i$ , for hadronic matter in ESC08Y and SU(3)Y, which is defined as  $Y_i = \rho_i/n_B$  with  $\rho_i$  being the number densities of particle species  $i = B, \ell$ . The upper panel (a) is for the case of ESC08Y, and the lower panel (b) is for the case of SU(3)Y. The thick vertical line shows the density at which a neutron star reaches the maximum-mass point by solving the TOV equation.

In contrast, in ESC08Y, we adopt the values of  $(g_{\omega N}, g_{\rho N})$  presented in Table IV of Rijken et al. (2010) in the calculation of coupling constants for hyperons. The couplings related to the hyperons are listed in Table 5.

### 5.2. Neutron Star Properties

The properties of neutron stars are, in general, estimated by solving the Tolman–Oppenheimer–Volkoff (TOV) equation (Oppenheimer & Volkoff 1939; Tolman 1939). Since the radius of a neutron star is remarkably sensitive to the EoS at very low densities, we use the EoS for nonuniform matter below  $n_B = 0.068 \text{ fm}^{-3}$ , where nuclei are taken into account using the Thomas–Fermi calculation (Miyatsu et al. 2013b).

In Figure 1, we illustrate the particle fractions for hadronic matter in ESC08Y and SU(3)Y. Although all other baryons are

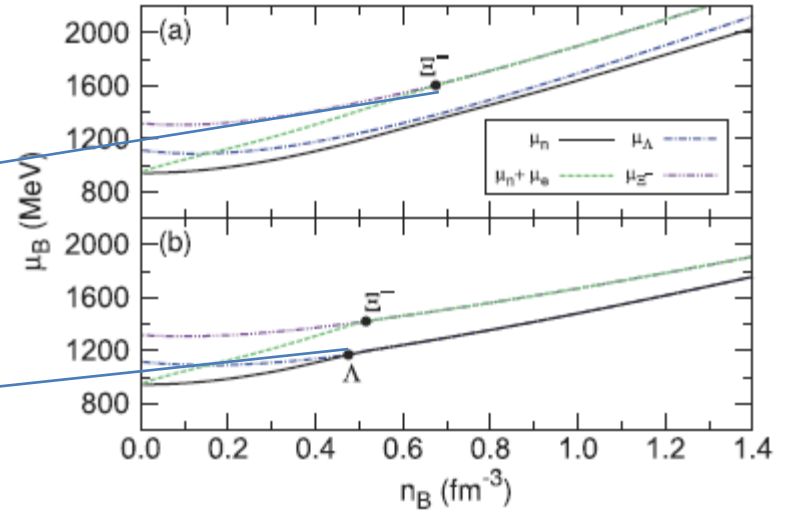


**Figure 2.** Chemical potentials for the  $n$ ,  $\Lambda$ ,  $\Xi^-$ , and  $e^-$  in ESC08Y and SU(3)Y. The filled circle denotes the onset of  $\Lambda$  or  $\Xi^-$ . The labels (a) and (b) are the same as in Figure 1.

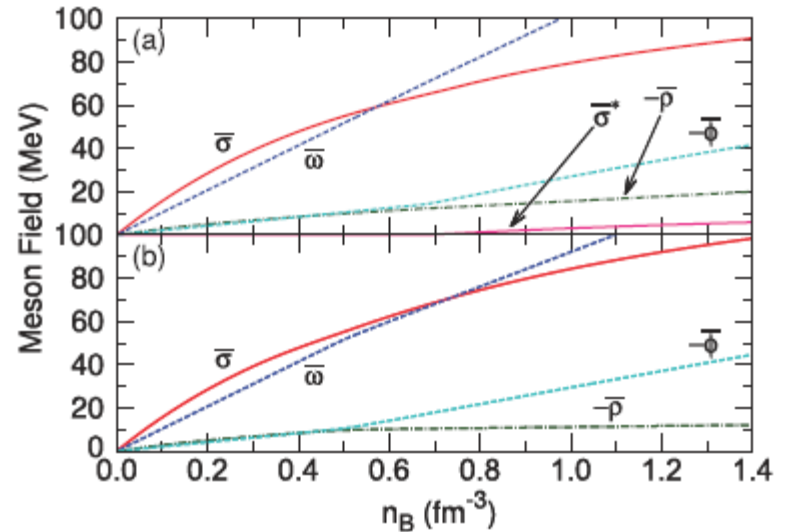


**Figure 3.** Meson fields in ESC08Y and SU(3)Y. The labels (a) and (b) are the same as in Figure 1.



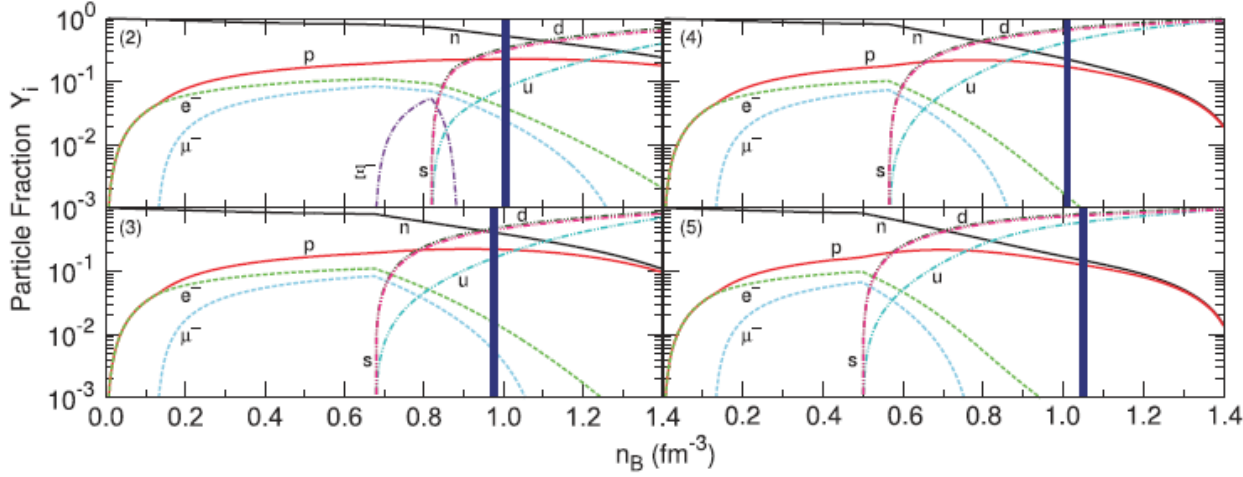


Figure 7. Particle fractions,  $Y_i$ , for hybrid-star matter in ESC08Y. The labels (2)–(5) designate the case number in Table 6.

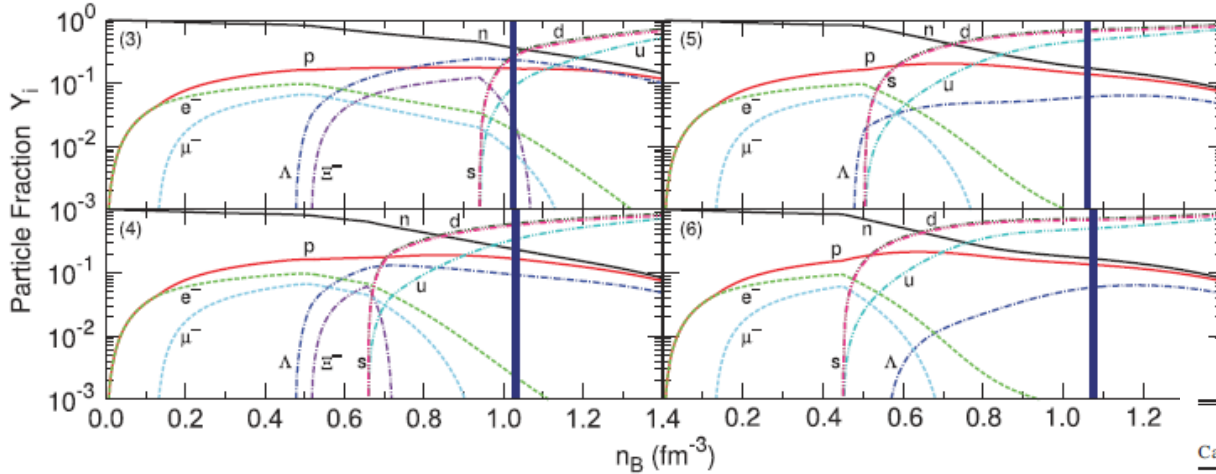
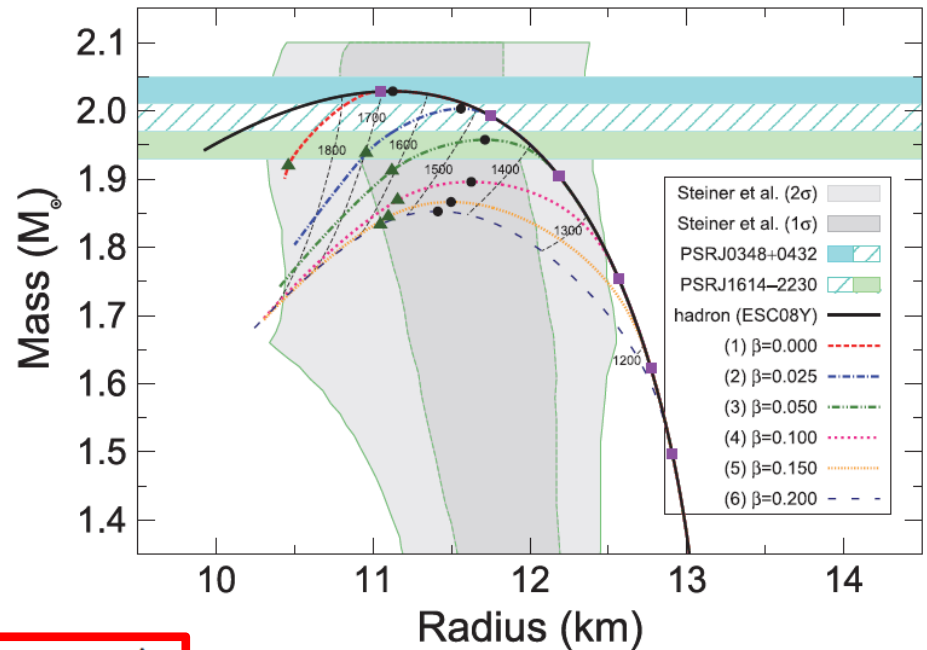
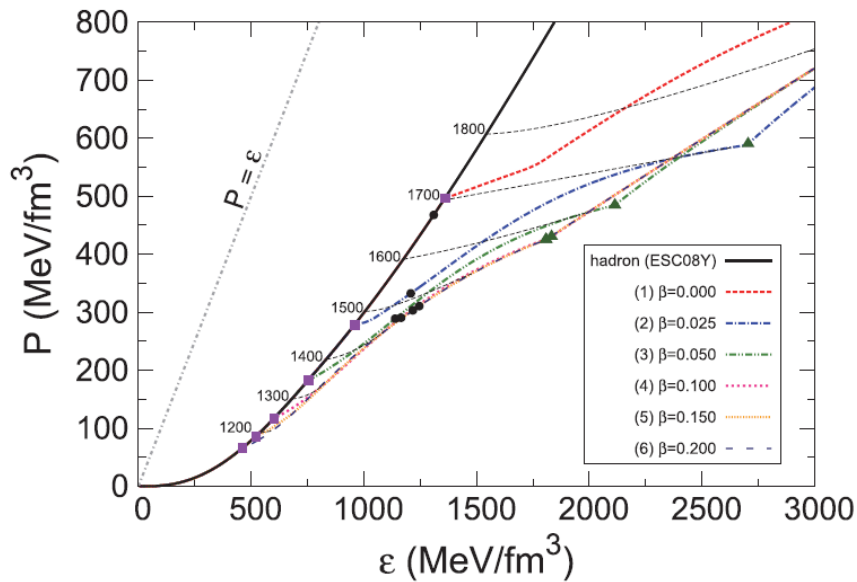


Figure 8. Particle fractions,  $Y_i$ , for hybrid-star matter in SU(3)Y. The labels (3)–(6) designate the case number in Table 6.

Table 6  
Phase Transition Properties at the Critical Density,  $n_B^{(c)}$  ( $\text{fm}^{-3}$ )

Case ( $\beta$ )	ESC08Y			SU(3)Y		
	$n_B^{(c)}$	$B^{(c)}$	$\mu_B^{(c)}$	$n_B^{(c)}$	$B^{(c)}$	$\mu_B^{(c)}$
(1) 0.000	1.065	400	1702	1.775	400	2031
(2) 0.025	0.820	224	1474	1.185	131	1605
(3) 0.050	0.680	184	1350	0.945	105	1444
(4) 0.100	0.565	143	1246	0.660	107	1274
(5) 0.150	0.500	123	1188	0.505	121	1188
(6) 0.200	0.450	115	1147	0.450	115	1147

Note. We list six cases, where the parameter  $\beta$  varies between 0 and 0.2, for ESC08Y and SU(3)Y. The critical bag constant,  $B^c$ , and the critical chemical potential,  $\mu_B^{(c)}$ , which are in the unit of MeV, are calculated by Equation (47).



In Figure 9, we present the EoS for hybrid-star matter in ESC08Y. In general, the quark productions soften the EoS, as is well known. Increasing the parameter  $\beta$ , the EoS becomes softer because the threshold densities of the quarks move toward lower densities, as seen in Table 6 and Figure 7. Furthermore, the pure QP emerges at lower densities as the parameter  $\beta$  increases.

Mass-radius relations for hybrid stars in ESC08Y. The shaded regions are the same as in Figure 5. The filled circles, squares, and triangles represent the contours of the nucleon chemical potential as explained in Figure 9.

before the QP transition. In case (2) of ESC08Y, the maximum mass reaches  $2.003M_{\odot}$  even if quark matter appears in the core of a neutron star. Therefore, the present EoS for hybrid-star matter can reasonably explain the recent mass constraint from astrophysical observations even if hyperons and quarks are included. As the properties of hybrid stars in SU(3)Y are

Case ( $\beta$ )
(1) 0.000
(2) 0.025
(3) 0.050
(4) 0.100
(5) 0.150
(6) 0.200

**Note.** We list the neutron-star radius,  $R_{\max}$  (in km), the ratio of the neutron-star mass to the solar mass,  $M_{\max}/M_{\odot}$ , and the central density,  $n_c$  (in  $\text{fm}^{-3}$ ), at the maximum-mass point.

# Contents

## 0. Introduction

### 1. A Hybrid model for Neutron Star

#### 1-1. Many-Body Interactions in Dense Matter

#### 1-2. Hyperon Puzzles of Neutron Stars

#### 1-3. Pomeron Exchange Model with SHF sets of Neutron Stars

### 2. Tidal Deformation from GW by Neutron Star Merge

#### 2-1. Tidal Deformation from GW

#### 2-2. Results by Various Models for NS

### 3. Quark cluster star

#### 3-1. Quark Matter inside Neutron Star

#### 3-2. Quark Star and Quark Cluster Star

## 4. Summary and Conclusions

What process would bring about a quark star? (Intermediate)

“What process would bring about a quark star? How would that differ from a neutron star?”

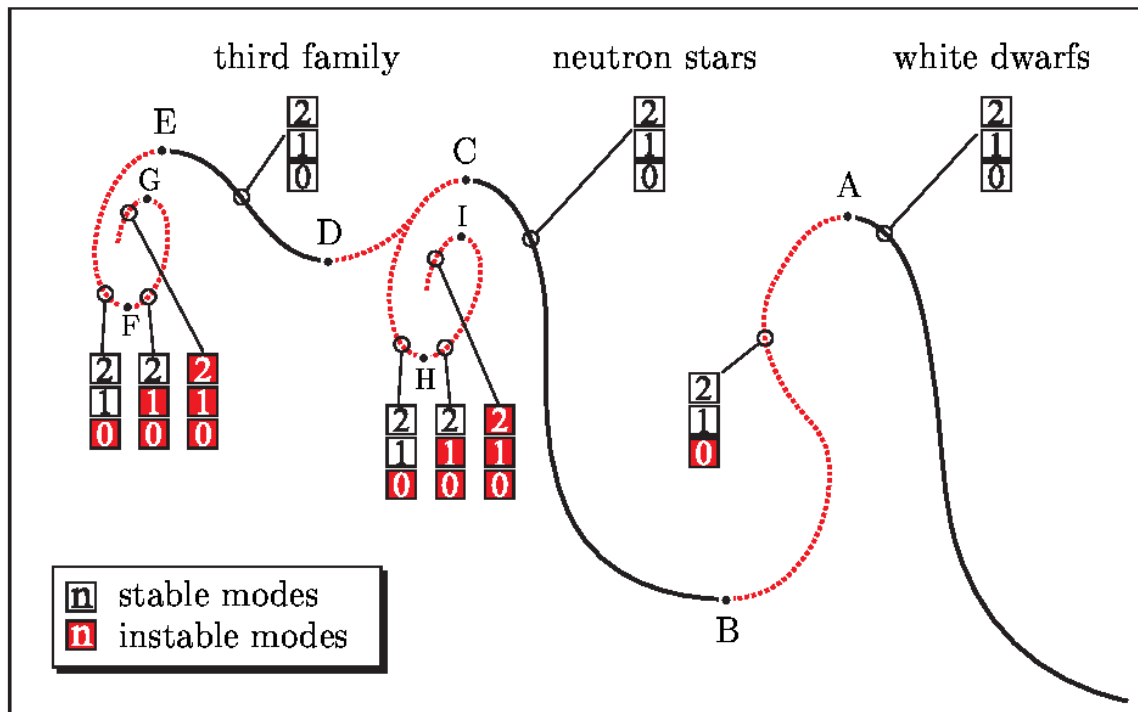
A neutron star is the remnant core of a massive, normal star after it has undergone a supernova explosion. It consists mostly of neutrons and is held up against gravitational collapse by "**neutron degeneracy pressure**" - this is a quantum mechanical effect that resists two neutrons being in the same place and therefore tends to push them apart when they get too close together.

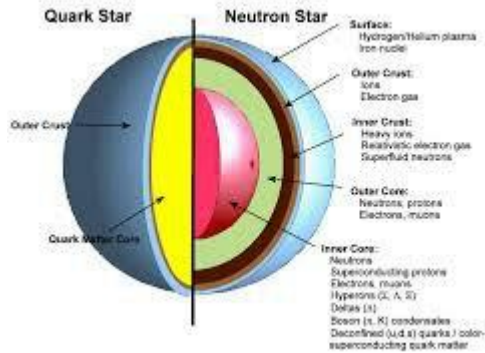
If the remnant core of the original star is massive enough (greater than a few times the mass of the sun) then the force of gravity will be stronger than the force of neutron degeneracy pressure and so the star will continue to collapse right on past the neutron star stage.

Currently, we think that the star will continue to collapse indefinitely past this point and eventually become a black hole. However, it is possible that there is another effect which comes into play - "**quark degeneracy pressure**". Quarks are the ultimate building blocks of protons and neutrons - each neutron is made up of three quarks - so it could be the case that as gravity overcomes neutron degeneracy pressure and causes the neutrons to "implode", the quarks put up some resistance of their own, and if the star isn't massive enough for its gravity to overcome that, then you would be left with a quark star instead of a black hole.

It is not yet known whether quark stars actually exist in nature because the details of what happens at such high densities are difficult to calculate. There has been some tentative evidence put forward for the existence of one quark star but it is by no means considered conclusive.







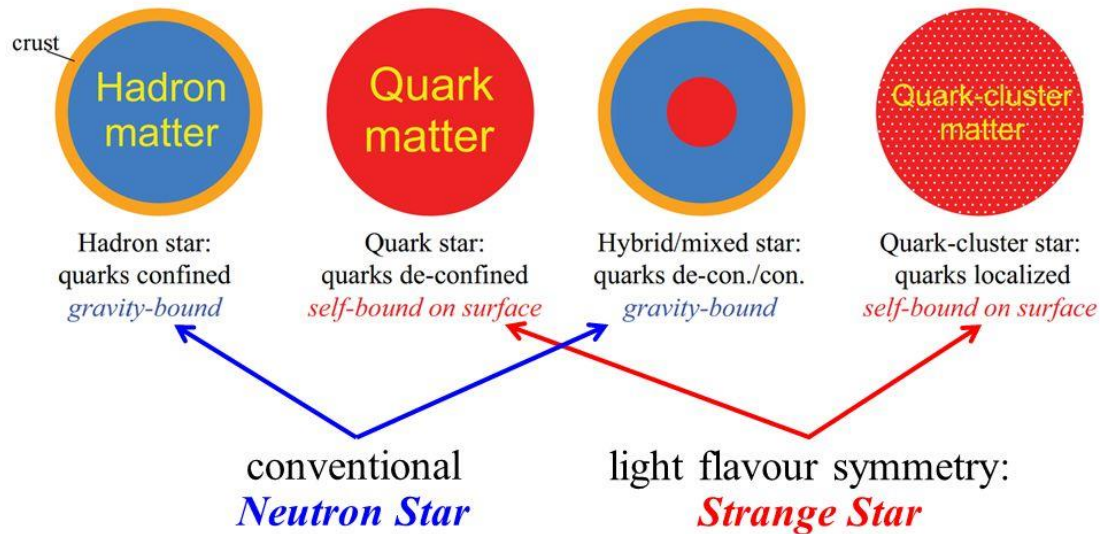
$$\frac{dP}{dr} = - \frac{[P(r) + \varepsilon(r)][M(r) + 4\pi r^3 P(r)]}{r[r - 2M(r)]}$$

## 4 Neutron star structure

With the evaluated hybrid star EOS presented in the last section we now turn to analyse the structure of the corresponding non-rotating neutron stars by solving the Tolman-Oppenheimer-Volkoff (TOV) equations [44]. These equations describe the balance between the gravitational force and the pressure given by the Fermi pressure of the particular EOS. This leads to a relation between the mass  $M$  and the radius  $R$  of the neutron star in general relativistic hydrostatic equilibrium.

# Observational hints from SM?

• **Pulsars**: different models in the market...

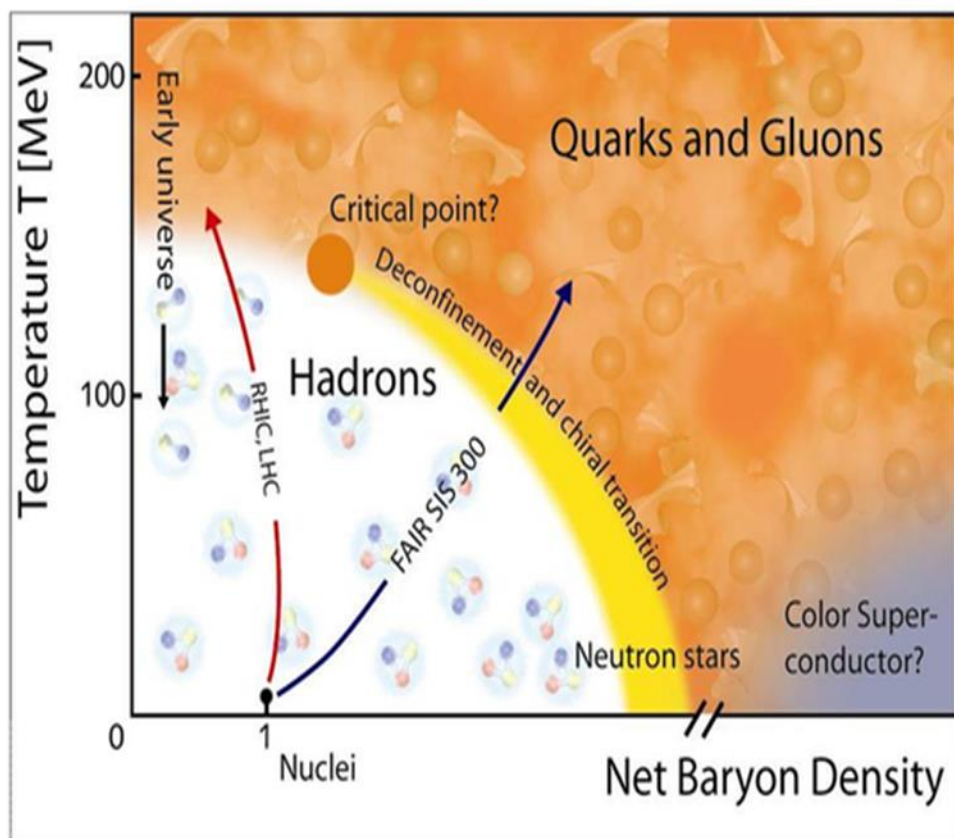


SN-nuclei

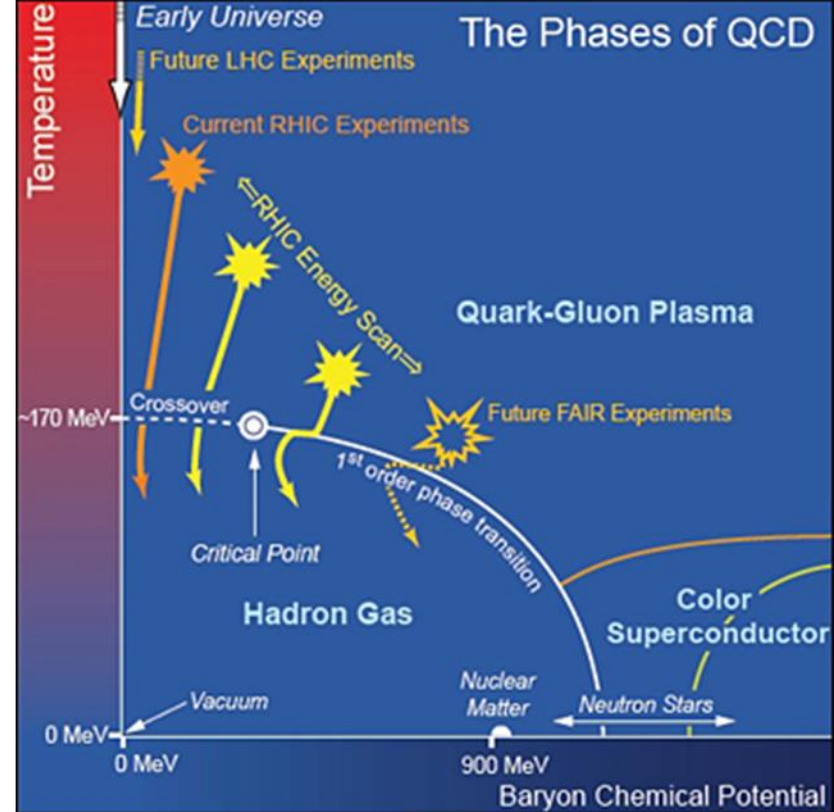
<http://www.phy.pku.edu.cn/~xurenxin/>

R. X. Xu

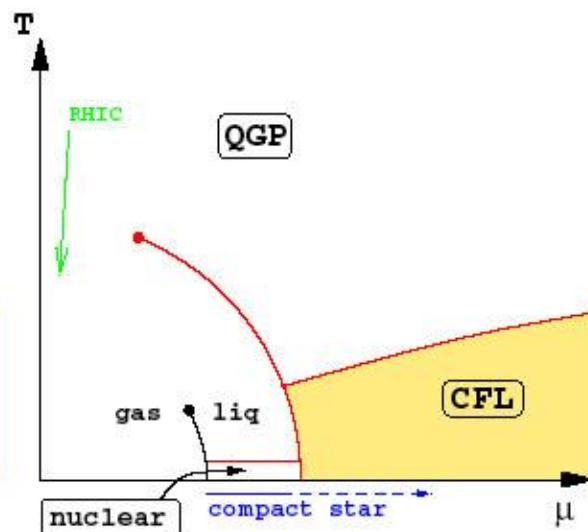
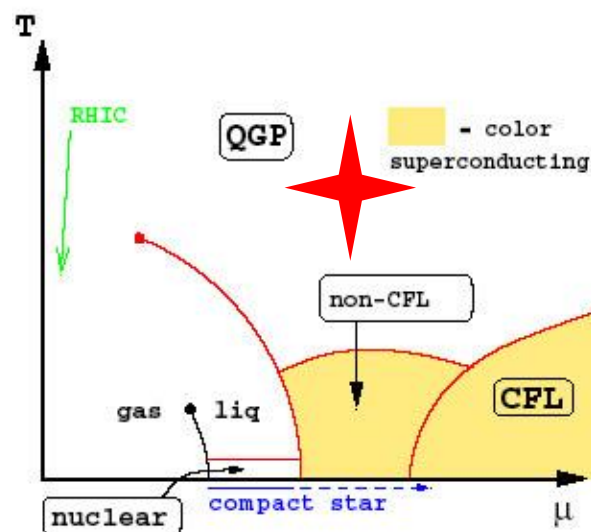
inner structure of pulsars. Traditionally speaking, quarks are confined in hadrons of neutron stars, while a quark star is composed of de-confined quarks. While a solid quark star is a condensed object of quark clusters, which distinguishes from conventional both neutron and quark stars (Xu 2003, 2010, 2013). The solid quark star (i.e. quark cluster star) is quite different from the traditional quark stars. The properties which are common in traditional quark stars, e.g. colour superconductivity with colour-flavour locking (Ouyed et al. 2006), are not expected in solid quark stars as the quarks in such stars cannot be treated as free fermion gas any more. The magnetic field of a solid quark star will also be quite different (Xu 2005) from that of a traditional quark star (Iwazaki 2005) because of the different magnetic origins (Xu 2005; Chen, Yu & Xu 2007).



Heavy strange quark



Light strange quark





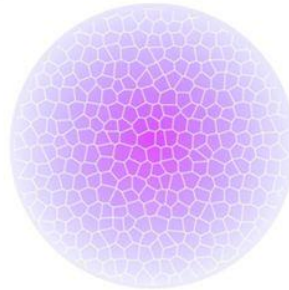
# EoS of compressed BM: specu. & obs.

- A quark-cluster star looks like a *big* metal ball

**Metal ball**

**V.S.**

**Quark-cluster star**

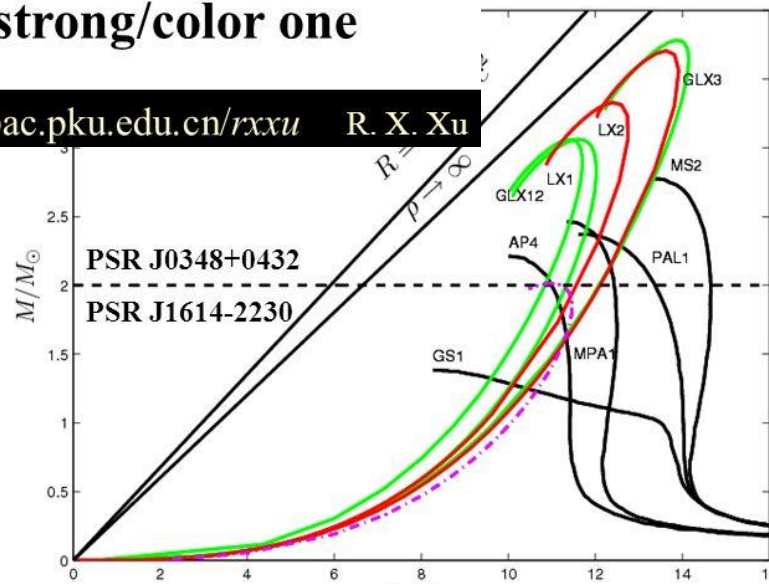


ions/nuclei  $\longleftrightarrow$  quark clusters

E-M interaction  $\longleftrightarrow$  strong/color one

**Evolution of States**

Compressed baryonic matter <http://vega.bac.pku.edu.cn/rxxu> R. X. Xu



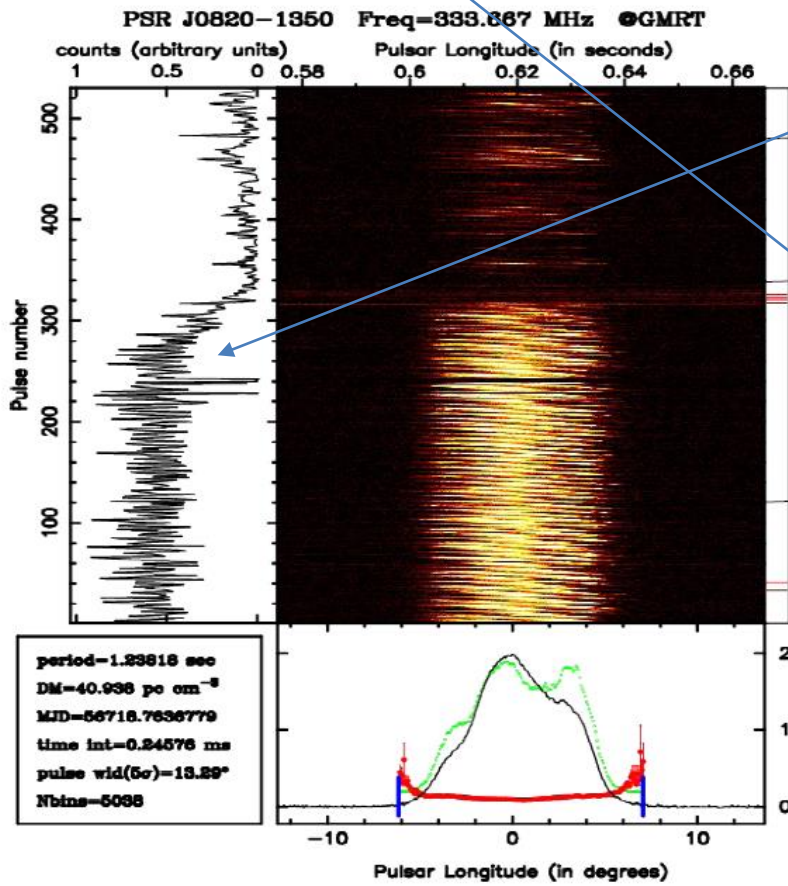
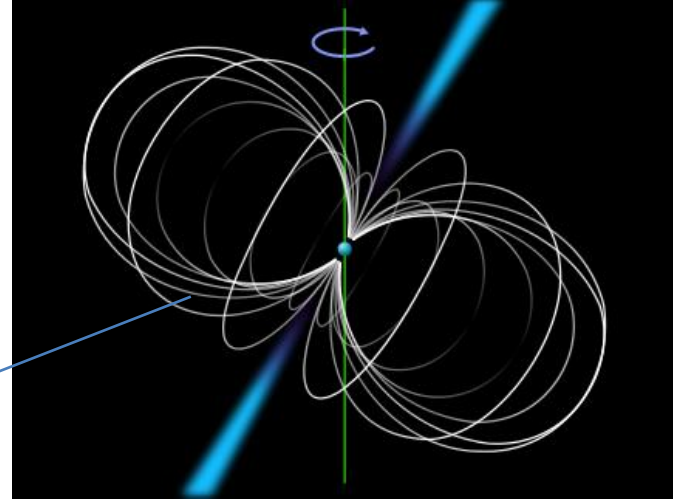
**Gravity bound**  
 Hadron star  
 Hybrid star  
 Hyperon Core  
 ( $R > 13$  km)  
 Fortin et al.(2014)

**Self-bound**  
 Quark star  
 Quark-cluster star

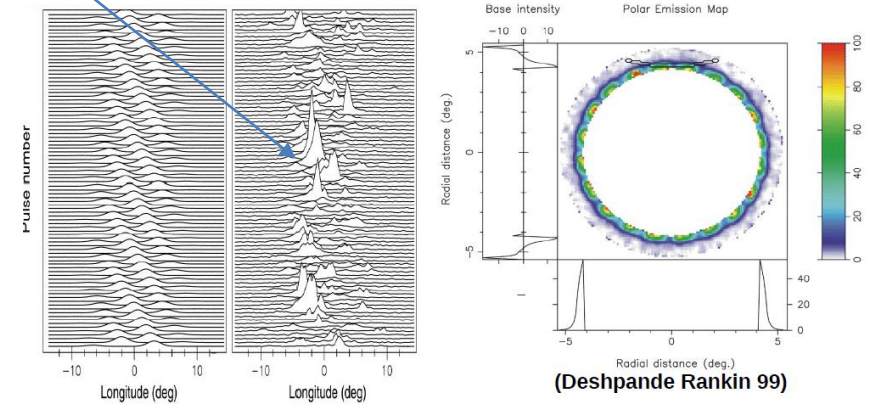
# Observational Data

## 1. Drifting subpulsar

# The Phenomenon

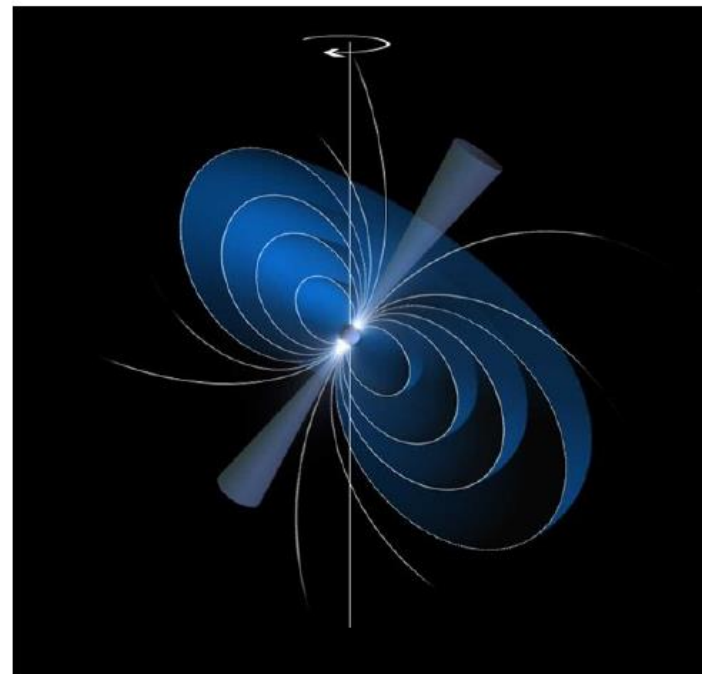
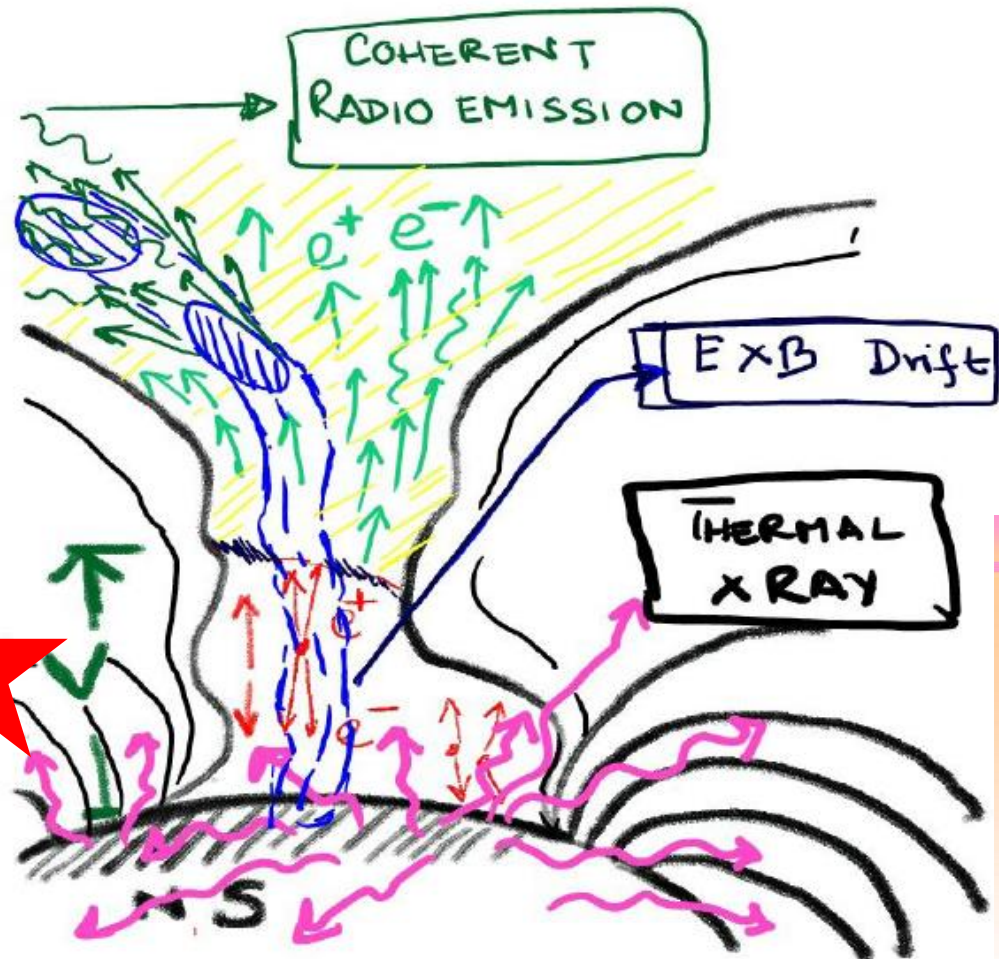


### The Case of PSR B0943+10

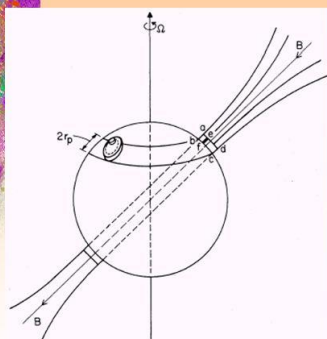


Explained by EXB drift of plasma (RS75)

# Xray/Radio emission



## Drifting sub-pulses



Accelerators:  
 • Inner vacuum gap (Ruderman & Sutherland 1975)

requiring high binding energy of charges on stellar surface

Xu, Qiao Zhang, 1999, ApJL, 522, L112

Deshpannde & Rankin, 1999, ApJ, 524, 1008

For drifting subpulsar, we need electric field or very high voltage between surface and outside. But normal NS could not produce enough E field compared to quark solid star because of some charged particles (or nuclei) on the surface of normal NS.



# Observational Data

## 2. Another accelerating mechanism for SN explosion

142 *S. Dai & R. X. Xu*

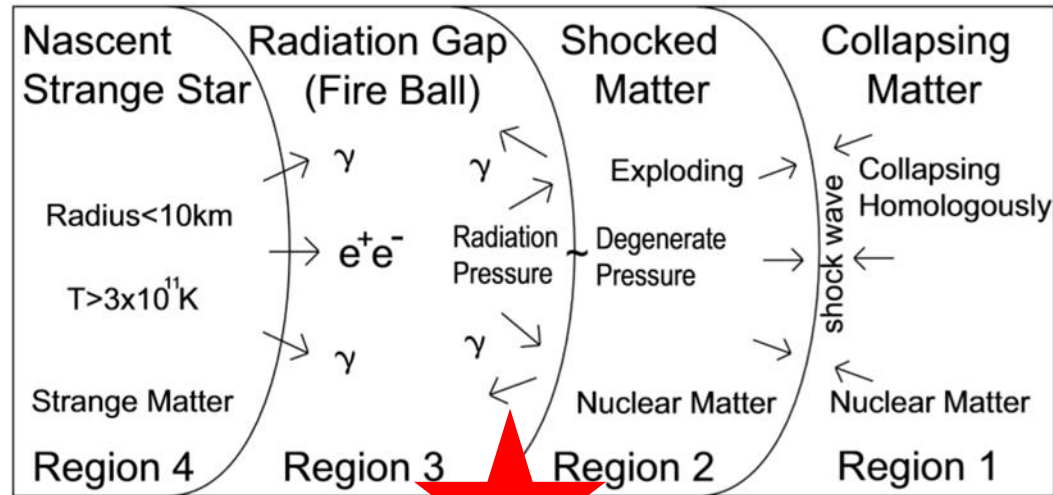


Fig. 2. An illustration of the photon-driven mechanism for core-collapse supernova (Chen et al. 2007). The outermost region 1 consists of the unshocked normal matter which is still in-falling, assembled to the homologous solution. Behind the shock front which serves as the border and increases in thickness, region 2 comprises the shocked nuclear matter whose motion has been reversed by the shock. Between the nascent strange quark-cluster star in the center of the original collapsing core and region 2 is a fireball (region 3), a gap filled up with high energy photons and  $e^+e^-$  pair plasma, similar to the fireball of gamma-ray bursts.



# Summary

## 1. **Tidal Deformation from GW** by Neutron Star Merge

1-1. Tidal Deformation from GW

1-2. **Results** by Various Models for NS

## 2. A Hybrid model for Neutron Star

2-1. **Many-Body Interactions in Dense Matter**

2-2. **Hyperon Puzzles** of Neutron Stars

2-3. **Pomeron Exchange Model with SHF sets of Neutron Stars**

## 3. Quark cluster star

3-1. Quark Matter inside Neutron Star

3-2. **Quark Star and Quark Cluster Star**





Thanks for your  
Attention !!